

# Fermion Doubling in Quantum Cellular Automata

Dogukan Bakircioglu, Pablo Arnault, and Pablo Arrighi

Université Paris-Saclay, INRIA, CNRS, ENS Paris-Saclay, LMF, 91190 Gif-sur-Yvette, France

A Quantum Cellular Automaton (QCA) is essentially an operator driving the evolution of particles on a lattice, through local unitaries. Because  $\Delta_x = \Delta_t = \varepsilon$ , QCAs constitute a privileged framework to cast the digital quantum simulation of relativistic quantum particles and their interactions with gauge fields, e.g.,  $(3 + 1)$ D Quantum Electrodynamics (QED). But before they can be adopted, simulation schemes for high-energy physics need prove themselves against specific numerical issues, of which the most infamous is Fermion Doubling (FD). FD is well understood in particular in the discrete-space but continuous-time settings of real-time/Hamiltonian Lattice Gauge Theories (LGTs), as the appearance of spurious solutions for all  $\Delta_x = \varepsilon \neq 0$ . We rigorously extend this analysis to the real-time discrete-space and discrete-time schemes that QCAs are. We demonstrate the existence of FD issues in QCAs. By applying a covering map on the Brillouin zone, we provide a flavoring-without-staggering way of fixing FD that does not break chiral symmetry. We explain how this method coexists with the Nielsen-Ninomiya no-go theorem, and illustrate this with a neutrino-like QCA.

## 1 Introduction

*Quantum cellular automata.* Quantum cellular automata (QCA) are shift-invariant causal unitary operators over lattices of quantum systems [4, 15]. They can always be realised as an infinitely repeating unitary quantum circuit, across space and time [2, 38]. As envisioned by Feynman right at the birth of Quantum Computing [16], they can be used for the digital quantum simulations of quantum field theories (QFTs). For this purpose, one tries and discretize the QFT in steps of  $\Delta_t = \Delta_x = \varepsilon$ . If successful, the wires of the circuit of the QCA will match the speed of light of the simulated QFT. For one step of time that is, because for a large number of time steps, the circuit's lightcone is squared-shaped—yet the round-shaped propagation of the simulated particles is faithfully reproduced [1]. Such relativistic models can even be shown shown to be Lorentz I covariant, as was done in three different ways [3, 9, 11]. This is in contrast with Hamiltonian-based quantum simulation [8, 27], which is fundamentally non-relativistic, and will remain so even once it gets digitalized after the facts into a QCA e.g. by means of a trotterization [25].

*Fermion doubling.* The classical simulations of QFTs has a long history. Discrete space-time formulations of QFTs, aka Lattice Gauge Theories (LGT), were formally introduced using the Lagrangian formalism by Wilson in [39]. A discrete space, continuous time reformulations of LGTs, back in the Hamiltonian formalism, was provided by Kogut and Suskind in [24]. They, however, noticed a strange behaviour in the dispersion relation of the fermionic lattice theory. Namely, they have observed spurious non-physical solutions persisting whenever  $\Delta_x \neq 0$  however small, which would inevitably pollute the numerics—this problem is referred to as fermion doubling (FD). In [24], they proposed to fix FD by placing the two different chiralities of the Dirac spinors into adjacent but different lattice sites—this solution is referred to as staggered fermions. On the other hand, Wilson also proposed to fix FD by adding a  $\varepsilon$ -dependent term with discretized second-order spatial derivatives (which implies twice as large a spatial neighborhood as the discretization of Dirac fermions), disappearing in the continuum limit—this solution is referred to as Wilson fermions. Unfortunately, both solutions break chiral symmetry, and this had fundamental consequences over the realisation of the internal symmetries in lattice. Afterwards this FD problem proven to be

a fundamental issue of discrete models of fermionic systems [17, 28, 29]. Any discrete model of fermionic system should face with this issue before producing numerical results, and QCA are no exception to that.

*The FD problem in QCA.* In recent years several aspects of numerical analysis of QCA-based models for QFT have been investigated [10, 33, 37].

The FD problem has been neglected, however, with the exceptions of [5] and [22]. However, for both of them, FD analysis was based on those conducted for discrete space continuous time formulations of LGTs in the Hamiltonian formalism—which falls short in the discrete space-time setting. In particular, this leads the authors of [5], to falsely conclude that FD does not occur in their model.

*Contributions.* In this paper, we develop a rigorous, general FD analysis method in order to assess the presence of in QCA as well as discrete space-time models in general. We apply it to the latest QCA models of QFT, namely the  $(1+1)$ -QED QCA [5] and the  $(3+1)$ -QED QCA [14]. Whilst QCA are comparatively less FD prone than their Hamiltonian counterparts, we prove that they do suffer the FD problem. We explain how to fix it, according to a general method, which can be interpreted geometrically as introducing a covering map on the Brillouin zone. In direct space, our solution amounts to *flavouring-without-staggering*. Interestingly, it does not break chiral symmetry. We fully described the FD-fixed, Flavoured-QCA versions of [5, 14]. These feature  $\mathbb{Z}_2$  and  $\mathbb{Z}_2 \times \mathbb{Z}_2 \times \mathbb{Z}_2$  flavour symmetries, respectively.

*Roadmap.* In Sec. 2, we provide a way to analyze of FD in discrete space discrete time formulations of fermionic systems. Then, in Sec. 3, we apply this analysis to the  $(1+1)$ -QED QCA and the  $(3+1)$ -QED QCA. We realise that both of them suffer the FD problem, albeit less severely than usual lattice fermion models. In Sec. 4, We fix the FD problem of these models by introducing flavour degrees of freedom, respecting the dynamics of the models, yielding us the flavoured versions of these QCA. In Sec. 5, we prove that the two solutions that we have proposed in Sec. 4, admit a geometrical understanding as the application of a covering map on their Brillouin zone. Lastly in Sec. 6, we discuss how our results fit together with the Nielsen Ninomiya no-go theorem, and show that it is possible to have a neutrino-like particles in a flavoured QCA.

## 2 Background on fermion doubling

This section aims to convey a generalized way of analysing and resolving FD on lattice models of QFTs, by means of a paradigmatic example. Here we are interested in discrete-space discrete-time formulation of QFTs unlike [24, 36], which is cast in discrete space but continuous time. We will not base ourselves on a Hamiltonian as they do. We will not base ourselves on a classical Lagrangian either, as in [34, 40]. Instead, our analysis will depart directly from a discretization of the equations of motion. We draw inspiration from the Green’s function based methods of [31, 35].

### 2.1 Equations of motions

Consider a two dimensional spacetime lattice,  $\Lambda^2$ , with a spacing  $\epsilon$ , where  $\Lambda^2 \subset \mathbb{R}^2$ . In the limit where lattice spacing becoming finer and finer, the lattice starts become like  $\mathbb{R}^2$ . Let  $(t, x)$  be the time and space coordinates over  $\mathbb{R}^2$ . One can express the elements of  $\Lambda^2$  by letting  $t = n\epsilon$  and  $x = k\epsilon$ , with  $n, k \in \mathbb{Z}$ . In QFT, fields are defined to be maps from a manifold, where physical objects live, to a  $d$ -dimensional complex vector space  $\mathbb{C}^d$ . Here we take the fermionic field on the lattice to be a map  $\psi : \Lambda^2 \rightarrow \mathbb{C}^2$  obeying a discretization of the Dirac equation. Recall that in the  $(1+1)$ D continuum, the Dirac equation for a fermionic field  $\psi(t, x)$  can conveniently be written as

$$(i\partial_t \mathbb{I}_2 + i\sigma_3 \partial_x - m\sigma_1)\psi(t, x) = 0, \quad (2.1)$$

where  $\mathbb{I}_2$  is  $2 \times 2$  identity matrix,  $\sigma_1, \sigma_3$  are Pauli matrices, and  $m$  is the mass. In order to obtain discretization of this, a first idea would be to trade partial derivatives with right lattice derivative, but this would break the hermicity of the momentum and energy operators  $i\partial_x, i\partial_t$  [31, 36]. Traditionally, one wants to keep the discretized momentum and energy operators to

remain hermitian, so that their spectrum remain real [26]. This is achieved by trading partial derivatives with symmetric finite differences:

$$\hat{p}\psi(t, x) = -i\partial_x\psi(t, x) \rightarrow \hat{p}\psi(n, k) := -\frac{i}{2\epsilon}(\psi(n, k+1) - \psi(n, k-1)) \quad (2.2)$$

$$\hat{E}\psi(t, x) = i\partial_t\psi(t, x) \rightarrow \hat{E}\psi(n, k) := \frac{i}{2\epsilon}(\psi(n+1, k) - \psi(n-1, k)). \quad (2.3)$$

It turns out that this yields, not only hermitian momentum and energy operators, but also hermitian equations of motion:

$$\frac{i\mathbb{I}_2}{2\epsilon}(\psi(n+1, k) - \psi(n-1, k)) + \frac{i\sigma_3}{2\epsilon}(\psi(n, k+1) - \psi(n, k-1)) - m\sigma_1\psi(n, k) = 0. \quad (2.4)$$

This overall hermicity could not have been achieved using right lattice derivative, as proven in App. A. We refer to this discretization procedure ‘the naive discretization scheme’.

## 2.2 Fourier analysis

Functions on  $\Lambda^2$  can be compactly Fourier decomposed due to the periodicity of the lattice under  $\vec{a}_1 = \vec{x}\epsilon$  and  $\vec{a}_2 = \vec{t}\epsilon$ , where  $\{\vec{t}, \vec{x}\}$  are orthonormal vectors. The reciprocal lattice vectors are then  $\vec{b}_0 = 2\pi\vec{t}/\epsilon$  and  $\vec{b}_1 = 2\pi\vec{x}/\epsilon$ , they generate the BZ  $\mathcal{B} = \{(E, p) \in [-\pi/\epsilon, \pi/\epsilon]^2\}$ , which is the integration domain of the Fourier expansion. The fermionic field on the lattice is Fourier decomposed as

$$\tilde{\psi}(E, p) = \epsilon \sum_{n=-\infty}^{\infty} \sum_{k=-\infty}^{\infty} \psi(n, k) e^{-ipk\epsilon + iEn\epsilon} \quad (2.5a)$$

$$\psi(n, k) = \epsilon \int_{-\pi/\epsilon}^{\pi/\epsilon} \frac{dE}{2\pi} \int_{-\pi/\epsilon}^{\pi/\epsilon} \frac{dp}{2\pi} \tilde{\psi}(E, p) e^{ipk\epsilon - iEn\epsilon} \quad (2.5b)$$

where  $p$  and  $E$  are canonical conjugates of  $x$  and  $t$  respectively, and  $\tilde{\psi}(E, p)$  is a map from  $\mathcal{B}$  to  $\mathbb{C}^2$ . After substituting Fourier expanded  $\psi(n, k)$  in Eq. (2.4), we obtain (details in App. B):

$$\int_{-\pi/\epsilon}^{\pi/\epsilon} \frac{dE}{2\pi} \int_{-\pi/\epsilon}^{\pi/\epsilon} \frac{dp}{2\pi} e^{ipk\epsilon - iEn\epsilon} \hat{D}_{\mathcal{B}}(E, p) \tilde{\psi}(E, p) = 0, \quad (2.6)$$

where

$$\hat{D}_{\mathcal{B}}(E, p) = (\mathbb{I}_2 \sin(E\epsilon) - \sigma_3 \sin(p\epsilon) - m\epsilon\sigma_1).$$

Under the limit  $\epsilon \rightarrow 0$  around the points  $E\epsilon \sim 0$ ,  $p\epsilon \sim 0$ , and using  $\sin(x) \sim x$  for  $x$  small, we see that  $\hat{D}_{\mathcal{B}}(E, p)/\epsilon$  converges to  $(\mathbb{I}_2 E - \sigma_3 p - m\sigma_1)$ , which matches the behaviour of the continuum Dirac Eq. (2.1). This is the reason why we will only consider the  $\hat{D}_{\mathcal{B}}(E, p)\tilde{\psi}(E, p) = 0$  solution to Eq. (2.6). After all Eq. (2.6) is the Fourier expansion of a zero function, and one solution is to take all coefficients to be zero. Other solutions may exist, but they are not considered in a Physics context [21].

## 2.3 Spurious solutions

This match with the continuum occurs around the points lying in the disk  $U_{(0,0)} = \{(E, p) \in \mathcal{B} : d((E, p), (0, 0)) \ll \epsilon^{-1}\}$  where  $d(x, y)$  is the usual Euclidean metric over  $\mathcal{B}$ , and  $\vec{E}, \vec{p}$  are the base vectors of  $\mathcal{B}$ . However, because  $\sin(\pi - x) = \sin(x)$  for  $x$  is small, the neighbourhoods  $U_{(s,r)} = \{(r\pi\epsilon^{-1} + p, s\pi\epsilon^{-1} + E) \in \mathcal{B} : (E, p) \in U_{(0,0)}\} \setminus U_{(0,0)}$  where  $r, s \in \{-1, 0, 1\}$  behave just like  $U_{(0,0)}$  as far as  $\hat{D}_{\mathcal{B}}$  is concerned. Wrapping up  $\mathcal{B}$  as the torus  $\mathbb{T}^2 = \mathbb{S}^1 \times \mathbb{S}^1$  given its periodic boundary conditions as in Fig. 1, makes it clear that the  $U_{(s,r)}$  are the neighbourhoods of the points  $\{(r\pi\epsilon^{-1}, s\pi\epsilon^{-1})\}$ .

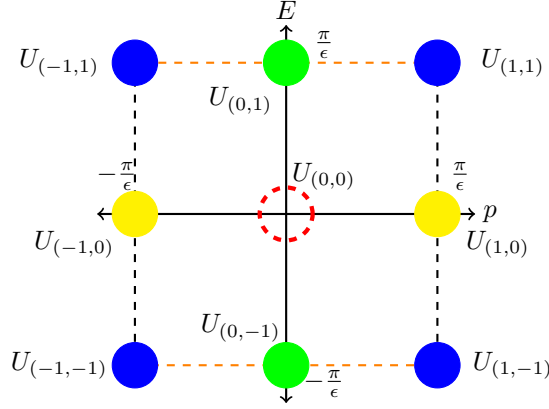


Figure 1: Fermion doubling neighbourhoods for the symmetric finite-differences scheme (yellow, green and blue) and for  $(1+1)$ -Dirac QW (blue only). The neighbourhoods having the same colour are in fact identical due to the toric geometry.

After this wrapping up, we see that there are three spurious  $U$ -disks, i.e. disks containing infinite energy and/or infinite momentum modes, that behave just like the finite modes lying in  $U_{(0,0)}$  that matches the solutions of the continuum. Intuitively, this is problematic, because this suggests that for arbitrary small  $\epsilon$ , these infinite modes will continue to behave just like legitimate solutions and pollute the numerics—only to vanish at exactly  $\epsilon = 0$  when they become ill-defined. But to formally decide if these infinite modes cause physical problems, let us look at the dispersion relation and the propagator of the discretized theory.

## 2.4 The dispersion relation

Consider the physical  $\hat{D}_{\mathcal{B}}(E, p)\tilde{\psi}(E, p) = 0$  solutions to Eq. (2.6). At coordinates  $(E, p)$  where  $\tilde{\psi}(E, p) \neq 0$ , this forces  $\det\{\hat{D}_{\mathcal{B}}(E, p)\} = 0$ . This condition is sometimes temporarily relaxed, in which case  $\tilde{\psi}(E, p)$  is said to be ‘off-shell’. For true aka ‘on-shell’ solutions, the support of  $\tilde{\psi}(E, p)$  i.e. its entire norm must therefore lie at

$$\det\{\hat{D}_{\mathcal{B}}(E, p)\} = (\sin^2(E\epsilon) - \sin^2(p\epsilon))/\epsilon^2 - m^2 = 0 \quad (2.7)$$

So, even though  $\tilde{\psi}(E, p)$  has domain the bidimensional  $\mathcal{B}$ , only the lines such that Eq. (2.7) matter, namely those meeting the ‘dispersion relation’.

The quantity  $\det\{\hat{D}_{\mathcal{B}}(E, p)\}$ , is referred to as the ‘dispersion’. It does not just serve to restrict the support of the on-shell solutions. It is a key physical quantity as we will now explain.

Indeed, in high energy experiments we are limited to certain physical observables, amongst which the propagator is the most essential. The propagator is the amplitude for a particle moving from  $(n, k)$  to  $(n', k')$ . Mathematically, it can be reformulated in terms of Green’s function  $G(n, k; n'k')$ , which is defined as follows:

$$\begin{aligned} \frac{i\mathbb{I}_2}{2\epsilon}(G(n+1, k; n'k') - G(n-1, k; n'k')) + \frac{\sigma_3}{2\epsilon}(G(n, k+1; n'k') \\ - G(n, k-1; n'k')) - m\sigma_1 G(n, k; n'k') = \delta(n-n')\delta(k-k'), \end{aligned}$$

So that

$$\psi(n, k) = \sum_{n'} \sum_{k'} G(n, k; n'k') \psi(n', k') \quad (2.8)$$

In Fourier space,

$$G(n, k; n'k') = \int_{-\pi/\epsilon}^{\pi/\epsilon} \frac{dE}{2\pi} \int_{-\pi/\epsilon}^{\pi/\epsilon} \frac{dp}{2\pi} e^{-ip(k'-k)\epsilon - iE(n'-n)\epsilon} G_{\mathcal{B}}(E, p), \quad (2.9)$$

where  $G_{\mathcal{B}}(E, p)$  is in general given the right inverse of the equation of motion in the sense of distributions [13]. In the context of the naive discretization [35] it suffices to ask  $\hat{D}_{\mathcal{B}}(E, p)G_{\mathcal{B}}(E, p) = \mathbb{I}_2$ , yielding, by the Cramer rule:

$$G_{\mathcal{B}}(E, p) = \frac{(\mathbb{I}_2 \sin(E\epsilon) + \sigma_3 \sin(p\epsilon) + m\epsilon\sigma_1)}{\det\{\hat{D}_{\mathcal{B}}\}}. \quad (2.10)$$

By just looking at Eq. (2.9), we see that the most significant contribution to the integral comes from the neighbourhoods of the zeroes of the denominator. In fact, these neighbourhoods of  $\mathcal{B}$  will be the only contributors to the integral in the continuum limit, as can be seen when the integral is turned into a complex contour integration [26]. In the continuum limit where  $\epsilon$  goes to zero, pairs  $(E, p)$  that make the denominator zero are the only ones that allow the propagation. Those are the only physically relevant  $(E, p)$  pairs. In fact, such pairs determine the space solution space of the Dirac equation: any solution must be a quantum superposition of the spacetime wavefunctions that correspond to these  $(E, p)$  pairs.

Similarly, the analysis of FD can be solely done in terms of the dispersion relation. Indeed, let us now take a more numerical point of view. Inspecting (2.10) we see that as  $\epsilon$  gets close to zero,  $G_{\mathcal{B}}(E, p)$  also gets close to zero except for the points in the neighbourhoods  $U_{(r,s)}$ , because the dispersion relation of Eq. (2.7) depends on  $(E, p)$  through the square of sin functions. As a consequence, all of the  $U_{(s,r)}$  contribute to the propagator just like  $U_{(0,0)}$  does, leading to overcounting.

In the exact continuum limit where  $\epsilon = 0$ , the Fourier space  $\mathcal{B}$  becomes  $\mathbb{R}^2$ . The points in the boundary of  $\mathcal{B}$  are no longer valid. Except for  $U_{(0,0)}$  the  $U_{(s,r)}$  are no longer defined. But we could still define some analogs of them by considering neighbourhoods of the  $p$ -axis, the  $E$ -axis, and the  $\pm p = \pm E$ -lines (and subtracting  $U_{(0,0)}$  from these sets). These neighbourhoods would again still be defined in the exact continuum limit where they would again lead to overcounting.

## 2.5 Resolution

In order to remove FD from the lattice formulation of fermions, one must seek to obtain a  $\sin p\epsilon/2$ ,  $\sin E\epsilon/2$  dependent  $\det\{D_{\mathcal{B}}\}$ , as  $\sin(x/2)$  is not symmetric under the transformation  $x \rightarrow \pi + x$ . Several methods have been used to do this, falling into two families. In the first family, the Dirac equation is modified additively [41] or multiplicatively [19], which necessarily breaks the chiral symmetry. In the second family, the lattice vectors are modified by  $1/$  choosing the Weyl representation of the Dirac equation and  $2/$  *staggering*, i.e. laying out the  $\psi^+$  and  $\psi^-$  components at different lattice sites [36], and  $3/$  *flavouring*, i.e. considering different sublattices as different particle species. The second step again breaks the chiral symmetry. This time, however, chiral symmetry breaking is not a necessity but a choice motivated by lattice quantum chromodynamics considerations [7]. Indeed, the no-go theorem of about chiral symmetry breaking on the lattice [29] only concerns chirally charged particles—as discussed this further in Sec. 6. Let us show that for Dirac particles, this does not have to be the case—essentially by skipping the staggering step  $2/$ .

In the second family of methods, one essentially seeks to implement a map  $\rho : \mathcal{B} \rightarrow \mathcal{B}^*$  such that  $(E, p) \mapsto (p', E') := (p/2, E/2)$ , so that  $\det\{D_{\mathcal{B}}\}$  depends on  $(\sin(p'), \sin(E'))$  instead: since  $\mathcal{B}^*$  is half of  $\mathcal{B}$ , the degeneracy due to the  $\pi$  symmetry will be avoided. But, what sort of map is this  $\rho$ ? Recall also that  $\mathcal{B}$  is the reciprocal space of  $\Lambda^2$ , from which it follows that  $\rho$  has a corresponding map at the level of the lattice, namely  $\rho^* : \Lambda^2 \rightarrow \Lambda_{(0,0)}^2$ , where  $\Lambda_{(0,0)}^2$  is the sublattice whose generating vectors are  $\{\vec{a}_1^*, \vec{a}_0^*\} = \{2\vec{a}_1, 2\vec{a}_0\}$ .

Notice that  $\Lambda^2$  has actually four such sublattices, i.e.  $\Lambda^2 = \Lambda_{(0,0)}^2 \cup \Lambda_{(1,0)}^2 \cup \Lambda_{(0,1)}^2 \cup \Lambda_{(1,1)}^2$ , where  $\Lambda_{(i,j)}^2 := \Lambda_{(0,0)}^2 + (i.a_0, j.a_1)$ . The solution is simply to ‘flavour them’, i.e. consider that they host different particle ‘species’. That way, we are effectively breaking the  $\{a_0, a_1\}$  lattice symmetry down to a  $\{\vec{a}_1^*, \vec{a}_0^*\}$  lattice symmetry.

Technically, the one-particle sector therefore got split into four distinguished sectors of different flavours:  $\psi_f : \Lambda_f^2 \rightarrow \mathbb{C}^2$ , where  $f \in \{(0,0), (1,0), (0,1), (1,1)\}$ . This  $f$  degrees of freedom is motivated by a global lattice symmetry arguments which the dynamics does not see. This justifies the use of the word ‘flavour’, as opposed to the word ‘colour’ which tends to be used for gauge-symmetry induced degrees of freedom and intervene in the dynamics.

Back to Fourier space, notice also that whilst  $\mathcal{B}$  had four neighbourhoods contributing to the propagator,  $\mathcal{B}^*$  has only one neighbourhood, but now we have four copies of it, one of each flavour. The resolution of FD did not change the size of the solution space, it just made it consistent with that of the continuum.

Notice that we have not changed the dynamics. What we have done, is changing the type of questions that can be asked, both in the discrete model and in the continuous regime. All questions asked now need to include flavour information. We can conclude that, endowed with this extra degree of freedom, both regimes fall into agreement.

We believe that this *flavouring-without-staggering* resolution of FD is very general. Here we started from a discrete space discrete time equation of motion. We could have started from a discrete space continuous time equation of motions. Either way, one counts the degeneracies of  $\det\{D_{\mathcal{B}}\}$  which do not vanish in the continuum limit, and defines a map  $\rho$  on the BZ (Brillouin zone) to leave them out of reach. This characterizes a first sublattice in direct space, whose number of distinct translates corresponds to the number of degeneracies. Each lattice is attributed a flavour.

Here, the equations of motions where obtained by discretizing, in a hermicity preserving manner, the equations of motions arising from a well-known quantum Hamiltonian. In different context, such equations may instead arise from some classical Hamiltonian as obtained by means of some discretization of Hamilton's equations, or from some classical Lagrangian by means of some discretization of Euler-Lagrange equations. Next, we will see that a similar method applies for a dynamics time discrete as prescribed by a unitary evolution.

### 3 Fermion doubling in QCA

We investigate Fermion Doubling on QCA models. We do it for the QCA models that appeared in [5] and [14]. These models give an algorithm to simulate QED, using local unitary quantum gates that evolve the states.

Actually, we only need to do it for the one-particle sector of these models. Indeed, FD is a problem that arises specifically in the one-particle sector of a fermionic system but it generates actual problems in the interacting multi-particle sector of the models. Let us clarify this point. If one considers non-interacting models, of one or several particles, the FD problem can simply be avoided by means of regularity assumptions. This is because if the initial wave function of a particle is smooth enough, it will remain so, and this can be used to establish convergence [6]. Once interaction is turned on, however, the initial smoothness may be jeopardized, and high frequency modes may appear, producing non-physical solutions even in the way a single particle propagates. Thus, the analysis of FD really takes us back to the one-particle sector to answer questions such as: *What goes wrong numerically, if high frequency modes are enabled? How can we fix those, without relying on regularity assumptions?*

#### 3.1 (1 + 1)-QED QCA

A (1 + 1)-dimensional QCA simulating QED has been described in [5]. Since FD is only a problem that only concerns with the free propagation of Dirac fermions, we can just turn-off the interaction term, falling back into the (1 + 1)-Dirac QW. In fact we can even focus on the one-particle sector, namely the (1 + 1)-Dirac QW. The states of this model, in the one particle sector, in Schrödinger picture, at time  $t = n\epsilon$  can be written as

$$|\psi(n)\rangle = \sum_k \psi^+(n, k) |k_+\rangle + \psi^-(n, k) |k_-\rangle, \quad (3.1)$$

where  $|k_{\pm}\rangle$  represents a basis state of position  $x = k\epsilon$  and chirality  $\pm$ . The functions  $\psi^{\pm}(n, k)$ , are from  $\Lambda$  to  $\mathbb{C}$ . When the rule for the unitary dynamics of the (1 + 1)-Dirac QW are applied to

$|\psi(t)\rangle$ , we obtain

$$\psi^+(n+1, k) = \cos(m\epsilon)\psi^+(n, k-1) - i \sin(m\epsilon)\psi^-(n, k) \quad (3.2)$$

$$\psi^-(n+1, k) = \cos(m\epsilon)\psi^-(n, k+1) - i \sin(m\epsilon)\psi^+(n, k), \quad (3.3)$$

where  $m$  is again the mass of the fermion and  $\epsilon$  the space-time discretization step. If we define  $\psi(n, k) = (\psi^+(n, k), \psi^-(n, k))^T : \Lambda^2 \rightarrow \mathbb{C}^2$ , and take the continuum limit, (3.2) and (3.3) converges to the Dirac Equation [5]. We write (3.2) and (3.3) in matrix form and thus this time we define the evolution equation as

$$\hat{U}_{QW}^1 \psi(n, k) = \begin{pmatrix} \cos(m\epsilon)\hat{S} & -i \sin m\epsilon \\ -i \sin m\epsilon & \cos(m\epsilon)\hat{S}^\dagger \end{pmatrix} \begin{pmatrix} \psi^+(n, k) \\ \psi^-(n, k) \end{pmatrix} = \begin{pmatrix} \psi^+(n+1, k) \\ \psi^-(n+1, k) \end{pmatrix}, \quad (3.4)$$

where  $\hat{S}, \hat{S}^\dagger$  are translation operators that acts on wave functions as  $(\hat{S}\psi)(n, k) = \psi(n, k-1)$  and  $(\hat{S}^\dagger\psi)(n, k) = \psi(n, k+1)$ . In the same manner we can define time translation operators  $\hat{T}, \hat{T}^\dagger$ , whose actions are  $(\hat{T}\psi)(n, k) = \psi(n-1, k)$  and  $(\hat{T}^\dagger\psi)(n, k) = \psi(n+1, k)$ . Eq. (3.4) put in the form of an equation of movement becomes

$$\begin{aligned} \hat{M}_{QW}^1 \psi(n, k) = \\ \begin{pmatrix} \cos(m\epsilon)\hat{S} - \hat{T}^\dagger & -i \sin m\epsilon \\ -i \sin m\epsilon & \cos(m\epsilon)\hat{S}^\dagger - \hat{T} \end{pmatrix} \begin{pmatrix} \psi^+(n, k) \\ \psi^-(n, k) \end{pmatrix} = 0. \end{aligned} \quad (3.5)$$

We can make contact with the naive discretization scheme of Subsec. 2.1 by taking the anti-hermitian part of Eq. (3.4) (and multiplying by  $i$  in order to preserve overall hermicity). Symmetric finite differences reappear:

$$\begin{aligned} & -\frac{i}{2}(\hat{M}_{QW}^{1\dagger} - \hat{M}_{QW}^1)\psi(n, k) \\ &= \begin{pmatrix} -i \cos(m\epsilon)(\hat{S} - \hat{S}^\dagger)/2 + i(\hat{T}^\dagger - \hat{T})/2 & -\sin(m\epsilon) \\ \sin(m\epsilon) & i \cos(m\epsilon)(\hat{S} - \hat{S}^\dagger)/2 + i(\hat{T}^\dagger - \hat{T})/2 \end{pmatrix} \begin{pmatrix} \psi^+(n, k) \\ \psi^-(n, k) \end{pmatrix} \\ &= \left( \cos(m\epsilon) \frac{i\sigma_3}{2\epsilon} (\hat{S}^\dagger - \hat{S}) + \frac{i\mathbb{I}_2}{2\epsilon} (\hat{T}^\dagger - \hat{T}) - \sigma_1 \frac{\sin m\epsilon}{\epsilon} \right) \psi(n, k) = 0. \end{aligned} \quad (3.6)$$

Hence we obtained

$$\begin{aligned} \frac{i\mathbb{I}_2}{2\epsilon}(\psi(n+1, k) - \psi(n-1, k)) + \cos(m\epsilon) \frac{i\sigma_3}{2\epsilon}(\psi(n, k+1) - \psi(n, k-1)) \\ - \sin(m\epsilon) \frac{\sigma_1}{\epsilon} \psi(n, k) = 0. \end{aligned} \quad (3.7)$$

This is almost what we had in the naive discretization of the Dirac equation in the Subsec. 2. In the massless case  $m = 0$ , we actually find that Eq. (2.4) coincides with (3.6). However, remember that Eq. (3.6) only contains the anti-hermitian part of Eq. (3.4). So, this raises hopes that (3.4) could be less degenerate, less FD error-prone than Eq. (3.6) and (2.4).

As we did in Subsec. 2.1 for the naive discretization scheme, we can also take the time to evaluate whether this (1+1)-Dirac QW can be expressed in terms of a hermitian energy and momentum operators. But notice that this is not necessary in order to analyse FD. Nor is it a worry in the QCA tradition, which focuses on unitarity rather than hermicity. The sole aim of the following parenthesis is to connect with the Lattice Gauge theory tradition.

Expressing a unitary evolution in terms of an energy operator is straightforward:  $\hat{U}_{QW}^1 = \exp\{-i\hat{E}_{QW}^1\epsilon\}$  for some hamiltonian  $\hat{E}_{QW}$ .

Isolating the momentum operator of the (1+1)-Dirac QW is more complicated and possibly non-standard. It makes sense to try and factorize away the mass term and see what remains. Let

$$\hat{U}_m^1 = \exp(-im\sigma_1) = \begin{pmatrix} \cos(\epsilon m) & -i \sin(\epsilon m) \\ -i \sin(\epsilon m) & \cos(\epsilon m) \end{pmatrix}.$$

We have

$$\hat{U}_{QW}^1 = \hat{U}_m^1 \hat{U}_{\hat{p}}^1 \quad (3.8)$$

where, using  $\exp(i\epsilon\hat{p})\psi(n, k) = \psi(n, k+1)$ ,

$$\hat{U}_{\hat{p}}^1 = \begin{pmatrix} \sin^2(\epsilon m) + e^{i\epsilon\hat{p}} \cos^2(\epsilon m) & \frac{1}{2}i(-1 + e^{i\epsilon\hat{p}}) \sin(2\epsilon m) \\ \frac{1}{2}i(-1 + e^{-i\epsilon\hat{p}}) \sin(2\epsilon m) & \sin^2(\epsilon m) + e^{-i\epsilon\hat{p}} \cos^2(\epsilon m) \end{pmatrix}.$$

Although  $\hat{U}_{\hat{p}}^1$  is not exactly a translation, we can still interpret as a discrete, unitary exponential of momentum. Indeed, as  $\epsilon \rightarrow 0$ , we have  $\hat{U}_{\hat{p}}^1 = \exp(i\epsilon\hat{p}\sigma_3)$ . The operator  $-i \log(\hat{U}_{\hat{p}}^1)$  is hermitian and may be understood as a discrete momentum.

Finally let us analyse FD for the (1+1)-Dirac QW. For this we again want to look at the continuum limit of the determinant of Eq. (3.4) in Fourier space. We move to Fourier space, by using Eqs. (2.5). Expectedly,

$$(\hat{S}\psi)(n, k) = \frac{\epsilon}{4\pi^2} \int_{-\pi/\epsilon}^{\pi/\epsilon} dE \int_{-\pi/\epsilon}^{\pi/\epsilon} dp \tilde{\psi}(E, p) e^{ipk\epsilon - iEn\epsilon} e^{-ip\epsilon} \quad (3.9)$$

$$(\hat{S}^\dagger\psi)(n, k) = \frac{\epsilon}{4\pi^2} \int_{-\pi/\epsilon}^{\pi/\epsilon} dE \int_{-\pi/\epsilon}^{\pi/\epsilon} dp \tilde{\psi}(E, p) e^{ipk\epsilon - iEn\epsilon} e^{ip\epsilon} \quad (3.10)$$

$$(\hat{T}^\dagger\psi)(n, k) = \frac{\epsilon}{4\pi^2} \int_{-\pi/\epsilon}^{\pi/\epsilon} dE \int_{-\pi/\epsilon}^{\pi/\epsilon} dp \tilde{\psi}(E, p) e^{ipk\epsilon - iEn\epsilon} e^{-iE\epsilon}. \quad (3.11)$$

Note that the integration domain is again ranges  $(E, p) \in \mathcal{B}$  the reciprocal of the  $\Lambda^2$  lattice coordinates. This time however they do not necessarily match spectrum of discretized momentum and Energy operators. We expand using Eq. (3.4):

$$\begin{aligned} & \frac{1}{4\pi^2} \int_{-\pi/\epsilon}^{\pi/\epsilon} dE \int_{-\pi/\epsilon}^{\pi/\epsilon} dp e^{ipk\epsilon - iEn\epsilon} \\ & \times \begin{pmatrix} \cos(m\epsilon)e^{-ip\epsilon} - e^{-iE\epsilon} & -i \sin m\epsilon \\ -i \sin m\epsilon & \cos(m\epsilon)e^{ip\epsilon} - e^{-iE\epsilon} \end{pmatrix} \begin{pmatrix} \tilde{\psi}^+(E, p) \\ \tilde{\psi}^-(E, p) \end{pmatrix} = 0. \end{aligned} \quad (3.12)$$

The determinant of the matrix above is

$$\mathcal{D}^1(E, p) = 1 + e^{-2iE\epsilon} - 2e^{-iE\epsilon} \cos(p\epsilon) \cos(m\epsilon), \quad (3.13)$$

In the Taylor expansion for a small  $\epsilon$  this becomes

$$\mathcal{D}^1(E, p) = -\epsilon^2(E^2 - p^2 - m^2) + \mathcal{O}(3), \quad (3.14)$$

where  $\mathcal{O}(3)$  represent terms containing  $\epsilon^3$  or higher degrees. Indeed, the zeroth and the first order of  $\epsilon$  disappear and we are left with higher orders. In the continuum limit  $\mathcal{D}^1(E, p)/\epsilon^2$  approaches to

$$-E^2 + p^2 + m^2. \quad (3.15)$$

which is indeed the dispersion relation of the continuous theory. Notice that unlike for the naive discretization, the modes  $(E, p \pm \pi/\epsilon)$ ,  $(E \pm \pi/\epsilon, p)$ , for  $E$  and  $p$  finite, do not pollute the continuum limit of the (1+1)-Dirac QW. Indeed, as  $\epsilon \rightarrow 0$ ,

$$\begin{aligned} \mathcal{D}^1(E, p \pm \pi/\epsilon) & \neq \mathcal{D}^1(E, p) + \mathcal{O}(\epsilon^2). \\ \mathcal{D}^1(E \pm \pi/\epsilon, p) & \neq \mathcal{D}^1(E, p) + \mathcal{O}(\epsilon^2). \end{aligned} \quad (3.16)$$

However for the modes  $(E \pm \pi/\epsilon, p \pm \pi/\epsilon)$ , even for  $E$  and  $p$  finite, we do have

$$\mathcal{D}^1(E \pm \pi/\epsilon, p \pm \pi/\epsilon) = -\mathcal{D}^1(E, p). \quad (3.17)$$

Hence the (1+1)-Dirac QW has spurious solutions due to the  $(E \pm \pi/\epsilon, p \pm \pi/\epsilon)$  symmetry. Altogether, we see that the (1+1)-Dirac QW is indeed less FD error-prone than the naive discretization

method. High momentum low energy modes are no longer problematic, and this has led to some mistaken claims that such QW are FD free [5]. Unfortunately, this is not quite the case: clearly the four neighbourhoods  $U_{(\pm 1, \pm 1)}$ , contribute to the propagator just like  $U_{(0,0)}$  does, leading again to over-counting, which will pollute the numerics. Fig.1 portraits the degeneracies. The **Red** circled neighbourhood  $U_{(0,0)}$  is the usual solution of the Dirac theory. Recall that it was polluted by three extra neighbourhoods  $U_{\{(r,s)\}}$  in the naive discretization. With the  $(1+1)$ -Dirac QW, it is only polluted by the **blue** neighbourhoods  $U_{(\pm 1, \pm 1)}$ .

### 3.2 $(3+1)$ -QED QCA

Again a  $(3+1)$ -dimensional QCA simulating QED has been described in [14], but since FD is only a problem that only concerns with the free propagation of Dirac fermions, we turn-off the interaction term, focus on the one-particle sector, and fall back into the  $(3+1)$ -Dirac QW.

The  $(3+1)$ -Dirac QW is a set of rules that describe the dynamics of a fermion in a three-dimensional lattice. It decomposes into substeps. Each substep, can be described by a quantum circuit of local gates and of finite depth, applied on qubits, whose excitations simulate fermionic matter. There are four substeps: three steps implementing propagation along each space dimension, and one step for the mass term. This model effectively replaces space-time with a four-dimensional orthogonal lattice,  $\Lambda^4$ , still with lattice spacing  $\epsilon$ . In each lattice site, there exist 4 qubits, and they correspond the occupation numbers for the four possible components of the Dirac spinor. In the one particle sector, using the Schrödinger picture, at a given time step  $n$ , the wavefunction  $|\psi^3(n)\rangle$  is of the form

$$\sum_{k,l,m} \psi_1(n, k, l, m) |1000\rangle + \psi_2(n, k, l, m) |0100\rangle + \psi_3(n, k, l, m) |0010\rangle + \psi_4(n, k, l, m) |0001\rangle. \quad (3.18)$$

Letting  $\psi(n, k, l, m) := (\psi_1(n, k, l, m), \psi_2(n, k, l, m), \psi_3(n, k, l, m), \psi_4(n, k, l, m))^T$ , the function  $\psi : \Lambda^4 \rightarrow \mathbb{C}^4$  is the fermionic wave function. When applying the unitary prescribed by the model [14], we obtain four equations, here condensed into one operator equation.

$$\hat{M}_{QW}^3 \psi(n, k, l, m) = 0, \quad (3.19)$$

where  $\hat{M}_{QW}^3 = \hat{U}_{QW}^3 - \hat{T}^\dagger$  with  $\hat{T}$  again the time translation and  $\hat{U}_{QW}^3$  is the unitary time evolution operator of the  $(3+1)$ -Dirac QW, as defined by the product of four sub-steps,

$$\begin{aligned} \hat{U}_{QW}^3 &= \hat{U}_m^3 \hat{U}_{p_x}^3 \hat{U}_{p_y}^3 \hat{U}_{p_z}^3, \\ \hat{U}_{p_z}^3 &= \exp\{-i\hat{P}_z \sigma_3 \otimes \sigma_3 \epsilon\}, \quad \hat{U}_{p_y}^3 = \exp\{-i\hat{P}_y \sigma_3 \otimes \sigma_2 \epsilon\}, \\ \hat{U}_{p_x}^3 &= \exp\{-i\hat{P}_x \sigma_3 \otimes \sigma_1 \epsilon\}, \quad \hat{U}_m^3 = \exp\{-im\sigma_2 \otimes \mathbb{I}_2 \epsilon\}. \end{aligned} \quad (3.20)$$

The sub-steps,  $\hat{U}_{p_x}^3, \hat{U}_{p_y}^3$  and  $\hat{U}_{p_z}^3$  generate the dynamical parts of the evolution operator, whereas  $\hat{U}_m^3$  generates the mass term.

Again, in the Lattice Gauge theory tradition one cares about expressing the numerical scheme to hermitian energy and momentum operators, whereas in the QCA tradition the focus is on overall unitarity. As regards energy, by unitarity we have, like for the  $(1+1)$ -Dirac QW,  $\hat{U}_{QW}^3 = \exp(-i\hat{E}_{QW}^3 \epsilon)$  for some  $\hat{E}_{QW}^3$ . As regards momentum, we clearly have that  $\hat{U}_{p_z}^3 = \exp\{-i\epsilon \hat{p}_z \sigma_3 \otimes \sigma_3\}$  is a partial translation arising as the exponential of the  $\hat{p}_z$  momentum, and similarly in the other directions.

Let us proceed to analyse fermion doubling. We start by expressing  $\hat{U}_{QW}^3$  in terms of translation operators

$$\begin{aligned} (S_x \psi)(n, k, l, m) &= \psi(n, k-1, l, m) \\ (S_y \psi)(n, k, l, m) &= \psi(n, k, l-1, m) \\ (S_z \psi)(n, k, l, m) &= \psi(n, k, l, m-1). \end{aligned}$$

This gives

$$\hat{U}_{QW}^3 = \frac{1}{4} S_x^\dagger S_y^\dagger S_z^\dagger \begin{pmatrix} (1+i)(S_x^2(1-iS_y^2)+S_y^2-i)c & (1+i)S_z^2(i(S_x^2+i)S_y^2+S_x^2-i)c \\ (-1+i)(iS_x^2(S_y^2+i)+S_y^2-i)c & (1+i)S_z^2(S_x^2(S_y^2-i)-iS_y^2+1)c \\ (1+i)(S_x^2(1-iS_y^2)+S_y^2-i)s & (1+i)S_z^2(i(S_x^2+i)S_y^2+S_x^2-i)s \\ (-1+i)(iS_x^2(S_y^2+i)+S_y^2-i)s & (1+i)S_z^2(S_x^2(S_y^2-i)-iS_y^2+1)s \\ (-1+i)S_z^2(S_x^2(S_y^2+i)+iS_y^2+1)s & (1+i)(i(S_x^2+i)S_y^2+S_x^2-i)s \\ (-1+i)S_z^2(iS_x^2(S_y^2+i)+S_y^2-i)s & (-1+i)(S_x^2(1+iS_y^2)+S_y^2+i)s \\ (1+i)S_z^2(S_x^2(1-iS_y^2)+S_y^2-i)c & (1+i)(S_x^2(-1-iS_y^2)+S_y^2+i)c \\ (1+i)S_z^2(S_x^2(S_y^2+i)-iS_y^2-1)c & (1-i)(S_x^2(1+iS_y^2)+S_y^2+i)c \end{pmatrix} \quad (3.21)$$

where  $s = \sin m\epsilon$ ,  $c = \cos m\epsilon$ .

As in the previous subsection, we wish to Fourier transform Eq. (3.19), according to:

$$\begin{aligned} \tilde{\psi}(E, p_x, p_y, p_z) &= \epsilon^2 \sum_{n,k,l,m=-\infty}^{\infty} e^{i(E n - p_x k - p_y l - p_z m)\epsilon} \psi(n, k, l, m) \\ \psi(n, k, l, m) &= \epsilon^2 \int_{-\pi/\epsilon}^{\pi/\epsilon} \frac{dE dp_x dp_y dp_z}{(2\pi)^4} e^{-i(E n - p_x k - p_y l - p_z m)\epsilon} \tilde{\psi}(E, p_x, p_y, p_z). \end{aligned} \quad (3.22)$$

The integration domain is now the four dimensional,  $\mathcal{B} \times \mathcal{B} := \mathcal{B}^2$ . The translations operators showing in Eq. (3.21) can be expressed in Fourier space as

$$S_x = e^{ip_x \epsilon}, \quad S_y = e^{ip_y \epsilon}, \quad S_z = e^{ip_z \epsilon}, \quad \hat{T} = e^{iE \epsilon} \quad (3.23)$$

Again we analyse FD by examining whether the determinant of  $\hat{M}_{QW}^3$  in the Fourier space,  $\mathcal{D}^3(E, p_x, p_y, p_z)$ , contains spurious solutions in the continuum limit. We have:

$$\begin{aligned} \mathcal{D}^3(E, p_x, p_y, p_z) &= \frac{1}{8} e^{-2i\epsilon(2E+p_x+p_y+p_z)} \left( e^{2i\epsilon E} \cos(2\epsilon m) \left( 8e^{2i\epsilon(p_x+p_y+p_z)} \right. \right. \\ &\quad \left. \left. + e^{4i\epsilon(p_x+p_y+p_z)} + e^{4i\epsilon(p_x+p_y)} + e^{4i\epsilon(p_x+p_z)} + e^{4i\epsilon p_x} + e^{4i\epsilon(p_y+p_z)} + e^{4i\epsilon p_y} + e^{4i\epsilon p_z} + 1 \right) \right. \\ &\quad \left. + 4 \left( -8(1+e^{2i\epsilon E}) \cos(\epsilon m) \cos(\epsilon p_x) \cos(\epsilon p_y) \cos(\epsilon p_z) e^{i\epsilon(E+2(p_x+p_y+p_z))} \right. \right. \\ &\quad \left. \left. + 2e^{2i\epsilon(E+p_x+p_y+p_z)} + 2e^{2i\epsilon(2E+p_x+p_y+p_z)} + e^{2i\epsilon(E+2p_x+p_y+p_z)} + e^{2i\epsilon(E+p_x+2p_y+p_z)} \right. \right. \\ &\quad \left. \left. + e^{2i\epsilon(E+p_x+p_y+2p_z)} + e^{2i\epsilon(E+p_x+p_y)} + e^{2i\epsilon(E+p_x+p_z)} + e^{2i\epsilon(E+p_y+p_z)} + 2e^{2i\epsilon(p_x+p_y+p_z)} \right) \right). \end{aligned} \quad (3.24)$$

For finite  $(E, p_x, p_y, p_z)$ , this only admits terms in  $\epsilon^4$  or higher orders of  $\epsilon$ . We have

$$\mathcal{D}^3(E, p_x, p_y, p_z) = \epsilon^4 (E^2 - p_x^2 - p_y^2 - p_z^2 - m^2)^2 + \mathcal{O}(5). \quad (3.25)$$

This coincides with the continuous theory. These finite momentum modes belong to the neighbourhood  $U_0 = \{q \in \mathcal{B}^2 : d(q, (0, 0, 0, 0)) < \epsilon^{-1}\}$ . However, as far as the formula for  $\mathcal{D}^3(E, p_x, p_y, p_z)$  concerned, the modes that are in the following neighbourhoods behave just the same:

$$\begin{aligned} U_f &= \{(f_t \pi \epsilon^{-1} + E, f_x \pi \epsilon^{-1} + p_x, f_y \pi \epsilon^{-1} + p_y, f_z \pi \epsilon^{-1} + p_z) \in \mathcal{B}^2 \\ &: (E, p_x, p_y, p_z) \in U_0\}, \text{ with } f \in \{(\pm, \pm, 0, 0), (\pm, 0, \pm, 0), (\pm, 0, 0, \pm), (0, \pm, \pm, 0), \\ &\quad (0, \pm, 0, 1), (0, 0, \pm, \pm), (\pm, \pm, \pm, \pm)\}. \end{aligned}$$

Even though the number of possible  $f$  is 40, they really correspond to 7 distinct neighbourhoods due to the boundary conditions of  $\mathcal{B}^2$ , as shown in Fig. 2 below. These seven extra neighbourhoods will again pollute the numerics.

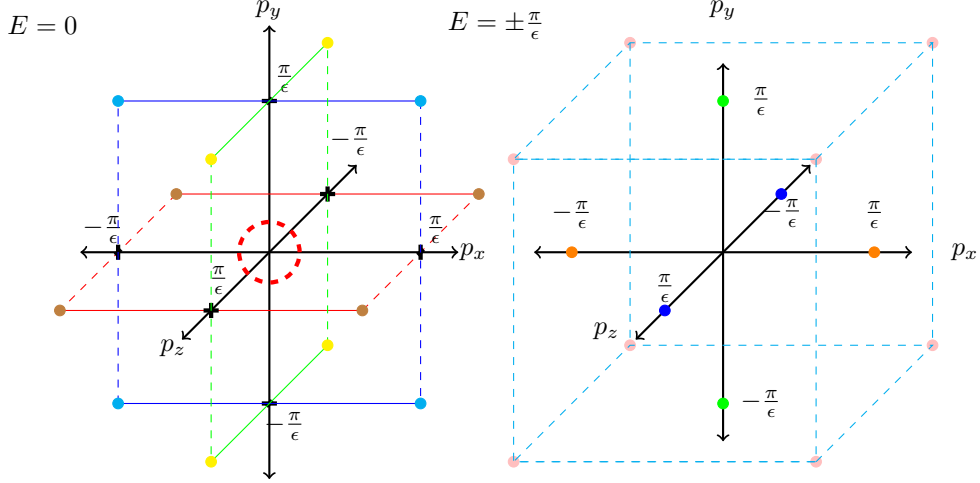


Figure 2: *Fermion doubling for the (3 + 1)-Dirac QW.* We draw the neighbourhoods on the hyper-surfaces where  $E = 0$  (left) and  $E = \pm\pi/\epsilon$  (right). The neighbourhood having the same colour are identical due to the toric geometry.

## 4 Solution of fermion doubling in QCA

Having demonstrated the existence of FD problems in (1 + 1)- and (3 + 1)-QED QCA, we now propose *flavouring-without-staggering* resolutions along the lines of Sec. 2. Recall that the method is to change the BZ in a way that avoids the FD neighbourhoods. As the BZ is defined by the reciprocal space lattice vectors, this points to a corresponding direct space lattice vectors, and hence a sublattice. Each translate of the sublattice needs a flavour.

### 4.1 (1 + 1)-QED QCA

Recall that FD occurs because of spurious relations arising the periodic nature of the dispersion relation, on its domain. For the (1 + 1)-QED-QCA model the symmetries are

$$\mathcal{D}^1(E, p) = \mathcal{D}^1(-\text{sgn}(E)\frac{\pi}{\epsilon} + E, -\text{sgn}(p)\frac{\pi}{\epsilon} + p) \quad (4.1)$$

where  $\{E, p\} \in \mathcal{B} = [-\pi/\epsilon, \pi/\epsilon] \times [-\pi/\epsilon, \pi/\epsilon]$ . We are going to avoid these symmetries simply by reducing the size of the domain. To achieve this, we need as in Fig. 3 to 1/ cut the BZ  $\mathcal{B}$  into regions that relate to one another by a translation, and 2/ colour them the same if  $\mathcal{D}^1$  acts the same upon them 3/ make sure that ‘pasting’ regions of the same colour on top of another places the FD neighbourhood on top of the original solution.

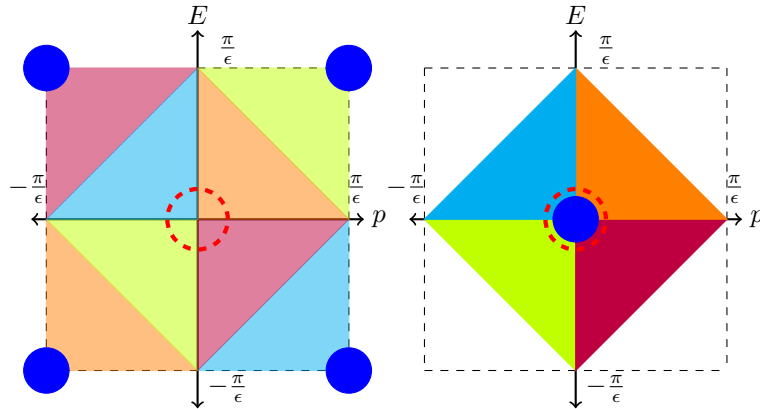


Figure 3: *Dispersion relations of the (1 + 1)-Dirac QW (left) and its flavoured version (right).* On the left, due to the periodicity  $\mathcal{D}^1(E, p)$ , the FD the neighbourhoods will pollute the continuum limit. On the right, the two-sheeted solution.

Fig. 3 is a solution with 8 regions and 4 colours. Notice that, as we cut the 4 triangles that are in the outside of the inner rhombus, and paste them on top of the rhombus, according to colours, we obtain the diagram on the right, whose opacity of the graph indicates the presence of the two sheets.

This procedure can be generalised and formalised in terms of Riemannian surface structure: we postpone this till Sec. 5.

Still informally for now, we observe that the procedure solves FD because there are no longer spurious solutions, but this is at the cost of having two-sheets, each contributing to the continuum limit. This will correspond to having **red** flavoured and **blue** flavoured fermions due to two sheets. Let us see how this works in practice. Restricting the BZ down to the rhombus changes its vectors to

$$\begin{aligned} b_0 &= \frac{\pi}{\epsilon} \vec{E} \rightarrow b'_0 = \frac{\pi}{2\epsilon} (\vec{E} + \vec{p}) \\ b_1 &= \frac{\pi}{\epsilon} \vec{p} \rightarrow b'_1 = \frac{\pi}{2\epsilon} (\vec{E} - \vec{p}) \end{aligned}$$

In terms of the direct space lattice vectors, this means changing  $\vec{a}_0 = \epsilon \vec{t}$  and  $\vec{a}_1 = \epsilon \vec{x}$  to  $\vec{a}'_0 = \epsilon \vec{t} + \epsilon \vec{x}$  and  $\vec{a}'_1 = \epsilon \vec{t} - \epsilon \vec{x}$ , as explained in App. C. But with these two lattice vectors only generate half the points of  $\Lambda^2$ , namely the 45 deg rotated orthogonal lattice  $\Gamma_r^2$ . We call  $\Gamma_b^2$  the lattice given by  $\Lambda^2 \setminus \Gamma_r^2$ . Notice that for  $r \in \Gamma_r^2$  and  $b \in \Gamma_b^2$ ,  $r = b + n_1 \vec{x} + n_2 \vec{t}$  when  $n_1 + n_2$  is an odd integer.

Both  $\Gamma_r^2$  and  $\Gamma_b^2$  admit the same rhombus shaped BZs,  $\tilde{\mathcal{B}}$ , with  $b'_0 = \frac{\pi}{2\epsilon} (\vec{E} + \vec{p})$  and  $b'_1 = \frac{\pi}{2\epsilon} (\vec{E} - \vec{p})$ . Thus each corresponds to one of the two-sheets.

We now distinguish these sublattices at the level of the state space, whilst keeping the (1 + 1)-Dirac QW dynamics as close as possible to the original one.

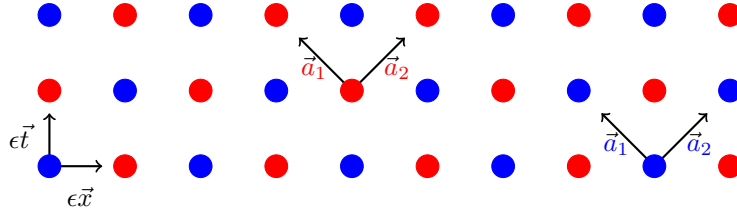


Figure 4: *Sublattices of the (1 + 1) Flavoured QCA.*

To do this we just add one qubit at each site  $(n, k)$ , and set it to **blue**  $= |0\rangle$  (resp. **red**  $= |1\rangle$ ) for even (resp. odd)  $n + k$ . We call this degree of freedom as ‘flavour’, because in particle physics, flavour is widely used to indicate degree of freedom caused by a global symmetry. Here it is just there to break the global symmetry. Flavour degrees of freedom traditionally do not intervene in the dynamics. The global symmetry corresponding to the flavour degree of freedom is  $\mathbb{Z}_2$ . Hence, we can easily expand the Hilbert space of (1 + 1)-D Dirac QW, with usual tensor product with 1-bit system,  $\{|0\rangle, |1\rangle\}$ .

For this flavoured lattice, at time  $t = n\epsilon$ , a state of (1 + 1)-Dirac QW in the one particle sector is of the form

$$|\psi(n)\rangle^f = \sum_k (\psi^+(n, k) |k_+\rangle + \psi^-(n, k) |k_-\rangle) \otimes (\sigma_x)^{n+k} |0\rangle. \quad (4.2)$$

i.e. the state of Eq. (3.1) tensored with the flavour,  $(\sigma_x)^{n+k} |0\rangle$ . Notice that we could have chosen a different convention, where the flavour is set to  $(\sigma_x)^{n+k} |1\rangle$ . In fact we could even have allowed for states that are superpositions of these two conventions, but the dynamics will be such that these sectors do not interfere with one another anyway. Indeed, the shifts within the dynamics need preserve this convention. Updating (1 + 1)-Dirac QW of Sec. 3.1 yields the flavoured QW

(FQW) with

$$\hat{S}^f = \hat{S} \otimes \sigma_x \quad (4.3a)$$

$$\hat{T}^f = \hat{S} \otimes \sigma_x \quad (4.3b)$$

$$\hat{U}_{FQW}^1 = \begin{pmatrix} \cos(m\epsilon)\hat{S}^f & -i \sin m\epsilon \\ -i \sin m\epsilon & \cos(m\epsilon)\hat{S}^{f\dagger} \end{pmatrix} \quad (4.3c)$$

$$\hat{M}_{FQW}^1 = \begin{pmatrix} (\cos(m\epsilon)\hat{S} - \hat{T}) \otimes \sigma_x & -i \sin(m\epsilon) \otimes \mathbb{I}_2 \\ -i \sin(m\epsilon) \otimes \mathbb{I}_2 & (\cos(m\epsilon)\hat{S}^\dagger - \hat{T}) \otimes \sigma_x \end{pmatrix} \quad (4.3d)$$

In order to check that FD is indeed resolved, let us look again at the determinant of  $M_{FQW}^1$  in Fourier space:

$$\mathcal{D}_f^1(E, p) = 4e^{-2i\epsilon E} (\cos(\epsilon E) - \cos(\epsilon m) \cos(\epsilon p))^2 \quad (4.4)$$

Notice that  $\mathcal{D}_f^1(E, p) = (\mathcal{D}^1(E, p))^2$ . It thus looks like the FQW has the same solutions as the original QW, but that is not the case, because its domain is smaller: the BZ of the FQW excludes the spurious solutions. Still the square captures the fact that the continuum limit is recovered not once, but twice. Indeed: we have traded our single fermion, that had spurious solutions, for two flavours of fermions with no spurious solutions. Note that the flavouring procedure can directly be applied to a multi particle sector of a QW, and one can obtain a flavoured-QCA.

*Interpretation of the resolution.* It may seem a bit paradoxical, at this stage, that just adding this extra qubit has solved the problem. This feeling is exacerbated in the massless case, where one notices that  $(1+1)$ -Dirac QW equations of motion of Eq. (3.5) was already compatible with restricting ourselves to the  $|0\rangle$ -flavoured sublattice  $\Gamma_b^2$  anyway, because if  $n+k$  is even so is  $(n \pm 1 + k \pm 1)$ . So in the massless case we did not even change the dynamics: by considering a  $|0\rangle$ -flavoured fermion we are really just restricting ourselves down to a sublattice. So, what have we really done remove to FD?

By restricting ourselves to one sublattice, we cut down the maximal frequency (both in space and in time) by a half. This removes fermion doubling. But putting both flavours back together one is of course allowed to prepare a seemingly fast oscillating state such as

$$|\psi(n)\rangle_{HF}^f = \sum_k (-1)^{n+k} (|k_+\rangle + |k_-\rangle) \otimes (\sigma_x)^{n+k} |0\rangle \quad (4.5)$$

which is the flavoured counterpart of

$$|\psi(n)\rangle_{HF} = \sum_k (-1)^{n+k} (|k_+\rangle + |k_-\rangle). \quad (4.6)$$

However, we now have that

$$|\psi(n)\rangle_{HF}^f = \sum_{k+n \text{ even}} (|k_+\rangle + |k_-\rangle) \otimes |0\rangle - \sum_{k+n \text{ odd}} (|k_+\rangle + |k_-\rangle) \otimes |1\rangle \quad (4.7)$$

which is just the superposition of two different-flavoured plane waves.

## 4.2 $(3+1)$ -QED QCA

Again we go back to the Fourier-transformed determinant of the equations of motions of the  $(3+1)$ -Dirac QW, as given in Eq. (3.24), and identify the symmetries that are the causes of the spurious solutions:

$$\mathcal{D}^3(E, p_x, p_y, p_z) = \mathcal{D}^3(-\text{sgn}(E)\frac{\pi}{\epsilon} + E, -\text{sgn}(p_x)\frac{\pi}{\epsilon} + p_x, p_y, p_z) \quad (4.8a)$$

$$\mathcal{D}^3(E, p_x, p_y, p_z) = \mathcal{D}^3(-\text{sgn}(E)\frac{\pi}{\epsilon} + E, p_x, -\text{sgn}(p_y)\frac{\pi}{\epsilon} + p_y, p_z) \quad (4.8b)$$

$$\mathcal{D}^3(E, p_x, p_y, p_z) = \mathcal{D}^3(-\text{sgn}(E)\frac{\pi}{\epsilon} + E, p_x, p_y, -\text{sgn}(p_z)\frac{\pi}{\epsilon} + p_z) \quad (4.8c)$$

Note that the equations above are the analog of Eq. (4.1) for each spatial dimension. Then the symmetries of  $\mathcal{D}^3(E, p_x, p_y, p_z)$  can be visualized with the three copies of the Fig. 3, as seen in Fig. 5(left). In this figure we condense the three graphs into one by laying them on top of one another. Note that through the combinations of these symmetries, there actually exist 8 possible class of symmetry transformations in 8 distinct two dimensional planes. We opt to take only three of them as a base of the symmetry transformations for the sake of simplicity.

Notice that although the symmetry structure in each hyperplanes is the same, their FD neighbourhoods remain distinct and hence need bear different colors, as we had done for Fig. 2. We lined them up according to the order of the hyperplanes, i.e. **orange** comes first as it belongs to  $E - p_x$ , then **green** as it belongs to  $E - p_y$ , and finally **blue** as it belongs to  $E - p_z$ .

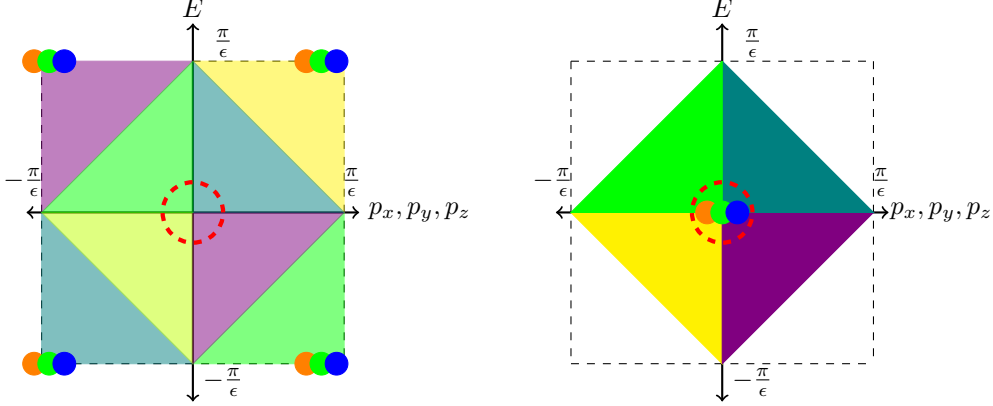


Figure 5: *Dispersion relations of the (3 + 1)-Dirac QW (left) and its flavoured version (right).* On the left, the FD neighbourhoods are projected on the hyperplanes,  $E - p_x, E - p_y, E - p_z$ . On the right, the eight-sheeted solution.

By observing Fig. 5 (left), we realise that the shrinking procedure of Subsec. 4.1 can be repeated for each hyperplanes independently, as illustrated by Fig. 5 (right). The formal treatment of the new BZ and the map that allows us to consider the sheeted structure has been discussed in Sec. 5. Still notice that these cutting and pasting procedures for three hyperplanes, induce cutting and pasting at the level of the other 2D hyperplanes,  $p_x - p_y, p_x - p_z$  and  $p_z - p_y$ , and similarly for the 3D hyperplanes etc. In the end the geometry of  $\mathcal{B}^2$  is again shrunk into a new BZ as hoped. Notice also that, cutting and pasting along  $E - p_x$  yields two sheets and lays the **orange** FD neighbourhood on top of the **red** correct continuum limit; next cutting and pasting along  $E - p_y$  yields four sheets and lays **green** FD neighbourhood on top of the correct continuum limit; and finally cutting and pasting along  $E - p_z$  yields us an 8-sheeted solution with all FD neighbourhoods on top of the correct continuum limit. This is because combinations of cutting and pasting procedures along these hyperplanes induce the same procedure on the hyperplanes that other FD neighbourhoods sit in Fig. 2. For example **brown** neighbourhoods sit in the  $p_y - p_z$  hyperplane as it is seen in Fig. 2, and by cutting along  $E - p_x$  and  $E - p_z$  results these **brown** neighbourhoods to be present in the origin point of the sheet that contains only the **brown** neighbourhoods.

These 8 sheet should be interpreted as 8 flavours arising from a global  $\mathbb{Z}_2 \times \mathbb{Z}_2 \times \mathbb{Z}_2$  symmetry. We can simply represent this flavour degree of freedom with 3 qubit system  $\{|000\rangle, |100\rangle, |010\rangle, |001\rangle, |110\rangle, |101\rangle, |011\rangle, |111\rangle\}$ . The first bit corresponds to the choice of sheet following  $E - p_x$  hyperplane cutting and pasting procedure, i.e. 0 for that carrying the **red** original continuum limit and 1 for that carrying the **orange** FD. The second bit corresponds to the choice of sheet following  $E - p_y$  etc. In direct space, where each flavour maps to one sublattice, it will be convenient to associate  $|000\rangle$  to the original  $\Gamma_{000}^4$  **red** sublattice, and  $|100\rangle$  to its  $x$ -shifted  $\Gamma_{100}^4$  **orange** sublattice, so that the flavoured  $x$ -shift is represented as  $S_x^f := S_x \otimes (\sigma_x \otimes \mathbb{I}_2 \otimes \mathbb{I}_2)$ . Similarly in the other spatial directions.

Following this logic one can establish a one-to-one correspondence between the sheet of the new BZ, the qubit encoding of its corresponding flavour, and the corresponding direct space sublattice

at time  $t = 0$ . We find:

$$\begin{aligned} \text{red} &\equiv |000\rangle, \quad \text{orange} \equiv |100\rangle, \quad \text{blue} \equiv |010\rangle, \quad \text{green} \equiv |001\rangle \\ \text{yellow} &\equiv |011\rangle, \quad \text{brown} \equiv |101\rangle, \quad \text{cyan} \equiv |110\rangle, \quad \text{pink} \equiv |111\rangle \end{aligned}$$

with the understanding that e.g. the **cyan** sublattice  $\Gamma_{110}^4$  is the  $(0, \epsilon, \epsilon, 0)$ -translate of the original **red** sublattice etc. This way we have deduced Fig. 6 (*middle*).

In direct space-time, after one time step and hence three substeps, a particle will have moved along the three directions and hence the flavoured time-translation needs be  $T^f := T \otimes (\sigma_x \otimes \sigma_x \otimes \sigma_x)$ . From this we deduce Fig. 6 (*left*) and (*right*).

Altogether, the 8 direct space-time lattices arising from the flavour symmetry,  $\mathbb{Z}_2 \times \mathbb{Z}_2 \times \mathbb{Z}_2$  form a covering of the four dimensional orthogonal lattice  $\Lambda^4$ ,

$$\Lambda^4 = \bigcup_{j \in \mathbb{Z}_2 \times \mathbb{Z}_2 \times \mathbb{Z}_2} \Gamma_j^4. \quad (4.9)$$

The exact correspondence between the generating vectors of these sublattices and the reciprocal vectors of the new BZ is detailed in App. C.2.

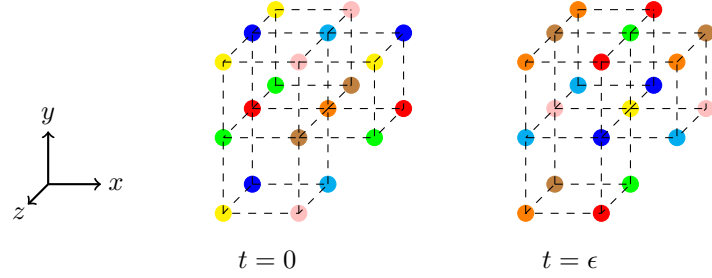


Figure 6: *Sublattices of the (3 + 1) Flavoured QCA.*

For this flavoured lattice, at time  $t = n\epsilon$ , a state of  $(3 + 1)$ -Dirac QW in the one particle sector,  $|\psi(n)\rangle^f$  is of the form

$$\begin{aligned} \sum_{k,l,m} (\psi_1(n, k, l, m) |1000\rangle + \psi_2(n, k, l, m) |0100\rangle + \psi_3(n, k, l, m) |0010\rangle \\ + \psi_4(n, k, l, m) |0001\rangle) \otimes ((\sigma_x)^{n+k} \otimes (\sigma_x)^{n+l} \otimes (\sigma_x)^{n+m} |000\rangle). \end{aligned} \quad (4.10)$$

The translation operators in space and time act also on the flavour degree of freedom, so as to respect Eq. (4.2) and Fig. 6:

$$S_x^f = S_x \otimes (\sigma_x \otimes \mathbb{I}_2 \otimes \mathbb{I}_2), \quad S_y^f = S_y \otimes (\mathbb{I}_2 \otimes \sigma_x \otimes \mathbb{I}_2) \quad (4.11a)$$

$$S_z^f = S_z \otimes (\mathbb{I}_2 \otimes \mathbb{I}_2 \otimes \sigma_x), \quad \hat{T}^f = \hat{T} \otimes (\sigma_x \otimes \sigma_x \otimes \sigma_x). \quad (4.11b)$$

We transform  $\hat{M}_{QW}^3$  to  $\hat{M}_{FQW}^3$ , just exchanging the translation operators with those above. Recall that  $\hat{M}_{FQW}^3$  is the generating operator of the equations of motions for  $(3 + 1)$ -FQW, which has the following form,

$$\hat{M}_{FQW}^3 = \hat{M}_{QW}^3 \otimes (\sigma_x \otimes \sigma_x \otimes \sigma_x). \quad (4.12)$$

Its determinant, in Fourier space,  $\mathcal{D}_f^3$  turns out to be:

$$(\mathcal{D}^3(E, p_x, p_y, p_z))^8. \quad (4.13)$$

We conclude that the number of solutions of the  $(3 + 1)$ -FQW is equal to that of the  $(3 + 1)$ -Dirac QW. I.e. we have 8 solutions, each of a different flavour, each coinciding with the continuum limit—instead of one good solution and 7 spurious solutions.

## 5 Flavouring is a covering map

Let us take a step back. To detect and fix FD, we 1/ started with some discrete Eq. of motion that produces the Dirac theory in continuum, 2/ transformed it into Fourier space, 3/ analysed its characteristic polynomial, 4/ observed that the polynomial had spurious solutions that would not vanish in the continuum limit 5/ Cut the domain of definition of the polynomial (aka BZ) into regions of similar behaviour, and “pasted them on top of each other” 6/ realized that these corresponded to sublattices in direct space 7/ flavoured each sublattice 8/ realised that, this way, each spurious solution has become a correct solution of a different flavour.

Now given such a BZ, and the FD neighbourhoods around the spurious solutions, in can be very difficult, in general, to understand which cutting and pasting procedure to apply in order to remove FD—namely step 5/ in the above suummary. We find that the best way is to visualize the BZ as a toric complex plane, and to come up with a covering map whose image is also a toric complex plane. In this section we will formalise this idea in the context of the  $(1+1)$ -Dirac QW and the  $(3+1)$ -Dirac QW.

### 5.1 $(1+1)$ -Dirac QW

We formalize the cutting and pasting procedures that we have done in previous section with the use of covering maps. Here is our strategy: first, we turn  $\mathcal{B}$ ,  $\mathcal{B}'$  into Riemann surfaces with complexification of the coordinates of  $\mathcal{B}$  and  $\mathcal{B}'$ , second we express  $\mathcal{B}$  as a complex torus which is the quotient of the complex plane by a square lattice, likewise we express  $\mathcal{B}'$  as a complex torus which is the quotient of the complex plane by an oblique lattice. Third, we define a map from the square lattice to the oblique lattice, fourth we prove that this map induces a covering map from  $\mathcal{B}$  to  $\mathcal{B}'$ .

To give the definition of a covering map, we simply repeat [18].

**Definition 1.** Suppose  $X, Y$  are topological spaces, a mapping  $p : Y \rightarrow X$  is called a covering map if every point  $x \in X$  has an open neighbourhood  $U$ , such that its preimage  $p^{-1}(U)$  can be represented as

$$\bigcup_{j \in J} V_j \quad (5.1)$$

where the  $V_j$  disjoint open subsets of  $Y$ ,  $j \in J$  where  $J$  is some discrete set. Moreover, all the mappings that are constrained on  $V_j$ ,  $p|_{V_j} \rightarrow U$  must be homeomorphisms.

Notice that the last sentence is not relevant in the context, as it concerns topologies that may have singularities.

Let us start by the first step, complexification of the coordinates of BZ by  $(E, p) \cong z = \epsilon(E + ip)/2\pi$ . Secondly, we find that the BZ of square lattice can be constructed by a quotient topology,  $\mathcal{B} \cong \mathbb{C}/\Lambda$ , where  $\Lambda = \{me^{2i\pi} + ne^{i\pi/2} : n, m \in \mathbb{Z}\}$ , meaning that  $z \sim z'$  if  $z - z' \in \Lambda$ . In Sec. 4, we worked out a way of departing from  $\mathcal{B}$  and arriving to the rhombus shaped  $\mathcal{B}'$ , which is also constructed by the quotient topology,  $\mathcal{B}' \cong \mathbb{C}/\Gamma^2$  with  $\Gamma^2 = \{(me^{-i\pi/4} + ne^{i\pi/4})/\sqrt{2} : n, m \in \mathbb{Z}\}$  and under the same complexification, as is clear from Fig. 3.

Notice that the lattice  $\Gamma^2$  characterises  $\mathcal{B}'$  and hence the map  $\varphi : \mathcal{B} \rightarrow \mathcal{B}'$  is characterised by  $v : \Lambda \rightarrow \Gamma^2$ . This map  $v$  is nothing but a multiplication by  $j = e^{-i\pi/4}/\sqrt{2}$ , as  $\Gamma^2 = j\Lambda$ . We would like to define  $\varphi$  with using the definition of  $v$ . We first define  $\varphi^* : \mathbb{C} \rightarrow \mathbb{C}$  on the all complex plane. Any complex number  $z'$  can uniquely be decomposed as  $z + \lambda$  with  $z \in \mathcal{B}$ ,  $\lambda \in \Lambda$ . We define  $\varphi^*(z')$  as

$$\varphi^*(z + \lambda) := z + j\lambda. \quad (5.2)$$

Next, we define  $\varphi(z) = \varphi^*(z + \lambda)/\Gamma^2$ . We have:

$$\begin{aligned} \varphi(z) &= (z + j\lambda)/\Gamma^2 = z/\Gamma^2 \quad \text{since } j\lambda \in \Gamma^2 \\ &= z - (mj + \frac{n}{2j}) \end{aligned} \quad (5.3)$$

for some  $n, m \in \mathbb{Z}$  that translate  $z$  in to  $\mathcal{B}'$ . We need to show that, for every open  $U \subset \mathcal{B}'$ ,  $\varphi^{-1}(U)$  is disjoint union of open subsets of  $\mathcal{B}$  so that we assure,  $\varphi$  is a covering map.

As is the case of these forms in general [12], it is clear that  $\varphi$  is not invertible, e.g.  $\varphi(0) = \varphi(j^{-1}) = 0$  and  $\varphi(\frac{e^{-i\pi/4}}{\sqrt{2}}) = \varphi(\frac{e^{5i\pi/4}}{\sqrt{2}}) = \frac{e^{-i\pi/4}}{\sqrt{2}}$ . Moreover for  $\varphi(0) \in U \subset \mathcal{B}'$ , we find  $\varphi^{-1}(U) = V_1 \cup V_2$ , where  $0 \in V_1$  and  $j^{-1} \in V_2$  are open neighbourhoods of  $\mathcal{B}$ . This is an example of  $U$  for which  $\varphi^{-1}(U)$  is a union of disconnected subsets of  $\mathcal{B}$ .

Nevertheless, the fact that  $\varphi$  is a two-covering needs to be proven. First we notice that  $\mathcal{B}' \subset \mathcal{B}$  and that the restriction of  $\varphi$  on  $\mathcal{B}'$  is the identity. For every  $z \in U \subseteq \mathcal{B}'$  we start with  $z = \varphi(z)$ ,  $z = \varphi(z') \neq z'$ ,  $z = \varphi(z'') \neq z''$ , where  $z \in V_1$ ,  $z' \in V_2$ ,  $z'' \in V_3$  and  $V_1, V_2, V_3$  are open neighbourhoods of  $\mathcal{B}$ . Let  $z' = z + 2hj + g/j$  and  $z'' = z + 2h'j + g'/j$ , where  $h, g, h', g' \in \{-1, 0, 1\}$  and  $h, g$  are chosen appropriately to keep  $z', z'' \in \mathcal{B}$ . For  $\varphi(z)$ , we get

$$\varphi(z') = z + (2h - m)j + \frac{2g - n}{2j} \quad (5.4)$$

for  $m = 2h$  and  $n = 2g$ , we find  $\varphi(z') = z$ . This proves that  $\varphi(V_2) = \varphi(V_1)$ . Moreover,  $z' - z'' = 2(h - h')j + (g - g')/j = 0$ , because otherwise  $z'' \notin \mathcal{B}$ , or  $z'' = z$ . Hence  $V_3 = V_2$ , we prove that  $\varphi$  is a two-covering map. The fact that  $\varphi$  is a two-covering between the BZ  $\mathcal{B}$  and  $\mathcal{B}'$  gives a geometrical understanding of FD as a  $\mathbb{Z}_2$  symmetry.

## 5.2 (3+1)-D Dirac QW

We would like to use the same reasoning as above for the  $(3+1)$  case, and show that the cutting and pasting procedure of Fig. 5 is an eight-covering map  $\varphi_2$  from  $\mathcal{B}^2$  to  $\mathcal{B}^{2'}$ . However here the four-dimensional  $\mathcal{B}^{2'}$ , is not a rhombus nor a cartesian product of rhombuses, rather it only admits a rhombus shape after a projection on a two-dimensional hyperplane is applied. For this reason, we have worked out a way of representing  $\mathcal{B}^{2'}$  as a Cartesian product of three  $\mathcal{B}$ 's in App. D. This makes use of the Bragg equation that allowed us to introduce degenerative representations of BZ. Namely, we found that  $\mathcal{B}^{2'} = \Pi \mathcal{B}'^3$  with  $\mathcal{B}'^3 = \mathcal{B}' \times \mathcal{B}' \times \mathcal{B}' \cong \mathbb{C}/\Gamma^2 \times \mathbb{C}/\Gamma^2 \times \mathbb{C}/\Gamma^2$  and  $\Pi$  a projection map. In the same manner,  $\mathcal{B}^2 = \Pi \mathcal{B}^3$  with  $\mathcal{B}^3 = \mathcal{B} \times \mathcal{B} \times \mathcal{B} \cong \mathbb{C}/\Lambda \times \mathbb{C}/\Lambda \times \mathbb{C}/\Lambda$  and  $\Pi$  the same projection. This  $\Pi$  takes  $(z, w, x) \in \mathbb{C}^3/\Lambda^3$  into

$$\Pi(z, w, x) = (\text{Re}(z) + i \text{Im}(w), \text{Im}(w) + i \text{Im}(x)). \quad (5.5)$$

Geometrically it must be understood as projecting upon the hyperplane  $\text{Re}(z) = \text{Re}(w) = \text{Re}(x)$ .

Now we can decompose the cutting and pasting procedures that we have in Fig. 5 as follows. First, we embed  $\mathcal{B}^2$  into  $\mathcal{B}^3$  as we have did in Fig. 5 (left) i.e. representing  $\mathcal{B}^2$  as a subset of the Cartesian product of three independent two-dimensional surfaces. Second, we define a covering map,  $\varphi_3$  from  $\mathcal{B}^3$  to  $\mathcal{B}'^3$ , just by letting  $\varphi_3 = \varphi \times \varphi \times \varphi$ , i.e.

$$\varphi_3(z, w, x) = (\varphi(z), \varphi(w), \varphi(x)) = (z - \gamma_0, w - \gamma_1, x - \gamma_2)$$

where  $\gamma_0, \gamma_1, \gamma_2 \in \Gamma^2$ . Due to Eq. (5.4), we see that  $\varphi_3$  is an eight-covering. Third, we apply the projection map  $\Pi$  so that the composite map  $\varphi_2 = \Pi \circ \varphi_3 \circ \Pi^{-1}$  maps  $\mathcal{B}^2$  to  $\mathcal{B}^{2'}$ . This  $\varphi_2$  remains an eight-covering map, because the multi valuedness of  $\Pi^{-1}$  gets cancelled by  $\Pi$ , as detailed in App. D.

## 6 Chiral Symmetry and no-go theorem

Here in this section, we show that the QCA models in [5, 14] are chirally symmetric. We also show that the flavoured version of these QCA models remain chirally symmetric. This may come as surprising to the more QFT inclined reader, with awareness of the famous no-go theorem by Nielsen and Ninomiya. We take an in-depth look at the relationship between this theorem and our flavoured-QCA models. This section may be skipped by the more quantum information inclined reader.

## 6.1 Chiral symmetry on Dirac QCAs

Although chirality is a well-known property of fermionic theories (see [26] for a comprehensive treatment), let us remind the reader of the definition in order to be self-contained.

Let us first observe the axial symmetry which allows us to define chirality. When we say that the  $(D+1)$ -Dirac equation, which is  $i\gamma^\mu \partial_\mu \psi(x^\mu) = 0$ , for  $\mu \in \{0, 1, \dots, D\}$ , is axially symmetric, we mean that  $i\gamma^\mu \partial_\mu (\exp\{i\theta\gamma^5\}\psi(x^\mu)) = 0$ , where  $\gamma^5 = i\gamma^0\gamma^1 \dots \gamma^D$ , hence  $[\gamma^5, \gamma^\mu] = 0$ .  $\gamma^5$  has two eigenvalues,  $\{1, -1\}$  and two corresponding eigenvectors  $\{\psi_R, \psi_L\}$ . They form the wave function, namely  $\psi = \psi_R + \psi_L$ . Hence  $\gamma^5\psi = \psi_R - \psi_L$ . The corresponding chiral projection operators are defined in the following form

$$\hat{P}_L = \frac{1}{2}(\mathbb{I}_{D+1} - \gamma^5), \quad \hat{P}_R = \frac{1}{2}(\mathbb{I}_{D+1} + \gamma^5).$$

They project the wave function into its left-handed,  $\psi_L$ , or right-handed,  $\psi_R$ , component, consequently the massless Dirac equation decouples into two equations, one for the left-handed component, and one for right-handed component: this fact is what is referred to as the chiral symmetry. Notice that, when  $\exp\{i\theta\gamma^5\}$  is applied on  $\psi_L$  and  $\psi_R$ , they take the phases  $\exp\{-i\theta\}$  and  $\exp\{i\theta\}$  respectively. We conclude that the essence of the axial symmetry is having two similar equations of motions whose wave functions take opposite orientations when a phase is applied.

Whilst axial symmetry and chiral symmetry often go hand-in-hand, this is not always the case (e.g. in the presence of weak interaction or Adler-Bell-Jackiw anomaly). In such cases we will not have axial symmetry but still we will have chiral symmetry. The massless Dirac operator,  $i\gamma^\mu \partial_\mu$  will commute with the chiral projection operators, and we will characterise chiral symmetry by means of this commutation relation.

Consider the  $(1+1)$ -QED QCA model in [5]. In the non-interacting case, it has continuum limit the  $(1+1)$ -Dirac eq. in the following representation:

$$(i\sigma_x \partial_t - \sigma_y \partial_x - m)\psi(t, x). \quad (6.1)$$

In this representation the chiral projection operators are

$$\hat{P}_L^1 = \frac{1}{2}(\mathbb{I}_2 - i\sigma_x \sigma_y), \quad \hat{P}_R^1 = \frac{1}{2}(\mathbb{I}_2 + i\sigma_x \sigma_y). \quad (6.2)$$

Even though these projection operators were defined in the continuum limit, they work unchanged in the discrete, as they do not depend on scaling  $\epsilon$ . The  $(1+1)$ -QED QCA is chirally symmetric theory, because the following commutation relation holds:

$$[\hat{M}_{QW}^1, \hat{P}_L^1] = 0, \quad [\hat{M}_{QW}^1, \hat{P}_R^1] = 0. \quad (6.3)$$

The unitary evolution operator of the  $(3+1)$ -QED QCA is written in the Weyl representation as we have seen in Eq. (3.20). The  $\gamma_W^5$  matrix in Weyl representation is

$$\begin{pmatrix} \mathbb{I}_2 & 0 \\ 0 & -\mathbb{I}_2 \end{pmatrix}$$

and the corresponding chiral projection operators are

$$\hat{P}_L^3 = \begin{pmatrix} 0 & 0 \\ 0 & \mathbb{I}_2 \end{pmatrix}, \quad \hat{P}_R^3 = \begin{pmatrix} \mathbb{I}_2 & 0 \\ 0 & 0 \end{pmatrix} \quad (6.4)$$

Again by checking the following commutation relations,

$$[\hat{M}_{QW}^3, \hat{P}_L^3] = 0, \quad [\hat{M}_{QW}^3, \hat{P}_R^3] = 0, \quad (6.5)$$

we establish that the  $(3+1)$ -QED QCA is chirally symmetric.

It is straightforward to see that if a QCA model is chirally symmetric, then its flavoured version is also chirally symmetric. This is because the chiral projection operators do not act on the flavour

degree of freedom. Let us display this fact on our flavoured version of  $(3 + 1)$ -QED QCA. The chiral projection operators for the flavoured theory are simply

$$\hat{P}_{FL}^3 = \hat{P}_L^3 \otimes \mathbb{I}_4, \quad \hat{P}_{FR}^3 = \hat{P}_R^3 \otimes \mathbb{I}_4.$$

Due to Eq. (4.12), we find

$$[\hat{M}_{FQW}^3, \hat{P}_{FL}^3] = 0, \quad [\hat{M}_{FQW}^3, \hat{P}_{FR}^3] = 0.$$

The same works for flavoured  $(1 + 1)$ -QED QCA is similar, they are also chirally symmetric. This means that for each flavour charge, we get decoupled left-handed, or right-handed fermions.

## 6.2 No-go theorem versus Flavoured QCA

Nielsen and Ninomiya's 1981 three papers about the constraints arising when putting chiral fermions on a lattice [28–30], are well-known in lattice QFT. Their no-go theorem is stated for the first time (first paper [29] p. 21) in the following terms:

“It is the purpose of this article to formulate and prove a *no-go theorem*: the appearance of equally many right- and left-handed species (types) of Weyl particles with given quantum numbers is an unavoidable consequence of a lattice theory under some *mild assumptions*.”

What is said in this passage, is that you need a state space that is able to handle as many left-handed as right-handed fermions at each site and for each every charge. One can prove that if one combines the left-handed and right-handed fermions into a single, massless Dirac fermion, then the model that evolves this massless Dirac fermion is chirally symmetric. This no-go theorem then seems to imply the following:

The most important consequence of our no-go theorem is that *the weak interaction cannot be put on the lattice*.

This is because the weak interaction requires the existence of neutrinos (left-handed fermions, charge  $-1$ ) and antineutrinos (right-handed fermions, charge  $0$ )—whose charges are different from each other—but right-handed neutrinos and right-handed antineutrinos have never been observed [20, 32].

Still, nothing forbids us from using a larger Hilbert space, e.g. capable of hosting right-handed neutrinos and right-handed antineutrinos, and simply not populating these particles. In fact, this can often be done quite elegantly by specifying a sector of the larger Hilbert space, as being the physical Hilbert space. After all, this is quite a common thing to do in quantum mechanics, e.g. think for instance of fermion parity sectors. One must of course make sure that the equations of motions leave the physical Hilbert space stable.

Now, in the Lattice QFT community, the question of potential loss of chiral symmetry, often gets mixed up with the FD issue [31].

“That the doubling phenomenon must occur in a lattice regularization which respects the usual hermiticity, locality and translational invariance requirements, follows from a theorem by Nielsen and Ninomiya [Nielsen (1981)] which states that, under the above assumptions, one cannot solve the fermion doubling problem without breaking chiral symmetry for vanishing fermion mass.”

Here the author seems to say that FD fixing, not just regularization, is also a source of chirality breaking. But this is only true of Wilson extra term techniques and staggering techniques, as these are clearly chirality breaking. Our flavouring-without-staggering technique is not chirality breaking.

Notice also that having introduced the flavour degrees of freedom into lattice, results in a richer structure under the no-go theorem. This is because the no-go theorem works in the Fourier space,

for each of the different sheets of  $\mathcal{B}'$ . For each sheet and for each possible charge, the dimension associated to the left-handed and right-handed fermions must be the same. When we switch back to direct space, we realise that the no-go theorem therefore applies independently for each flavoured sublattice. So, whilst each flavoured site must be able to carry an equal number of left-handed and right-handed fermions for every possible charge, different flavoured sites can still host different conserved charges.

By using this fact for flavoured lattice models, we will show that weak interaction in lattice under certain conditions while staying coherent with the no-go theorem is possible.

Let us combine all of these ingredients 1/ restricting ourselves to a sector of a larger Hilbert space, namely a physical Hilbert space which is left stable by the equations of motions and is 2/ neatly characterized by associating different charges and chirality occupancy to different flavours 3/ as arising from our flavouring-without-staggering method. The aim is to achieve an FD fixed, chirally symmetric model, which, in direct space, has just left-handed fermions of charge  $-1$  and right-handed fermions of charge  $0$ . We restrict ourselves to the massless case.

Take the  $(1+1)$ -FQW for  $m = 0$ . It has two flavours. Let the **red**  $\cong |0\rangle$  flavoured fermions have hypercharge  $0$  and the **blue**  $\cong |1\rangle$  flavoured fermions have hypercharge  $-1$ . From the no-go theorem we know that the large Hilbert space must cater for both both left-handed and right-handed particles for each flavour. In Fourier space, the vector field of the FQW at position  $(E, p)$  is given by the vector

$$\tilde{\psi}^\nu(E, p) = \tilde{\psi}_L^{\text{red}}(E, p) |-0\rangle + \tilde{\psi}_R^{\text{red}}(E, p) |+0\rangle + \tilde{\psi}_L^{\text{blue}}(E, p) |-1\rangle + \tilde{\psi}_R^{\text{blue}}(E, p) |+1\rangle$$

where  $\{+, -\}$  refers to chirality. It can be seen from Eq. (3.12), that the vectors  $\tilde{\psi}_L^T = (\tilde{\psi}_L^{\text{red}} \ \tilde{\psi}_L^{\text{blue}})$  and  $\tilde{\psi}_R^T = (\tilde{\psi}_R^{\text{red}} \ \tilde{\psi}_R^{\text{blue}})$  indeed correspond to the vector fields of the left-handed and right-handed fermions, respectively.

Consider  $\tilde{\psi}^\nu(E, p)$  a solution of the  $(1+1)$ -FQW. Since  $m = 0$ , the dispersion relation Eq. (2.7) simplifies to  $E = \pm p$ , so  $\tilde{\psi}^\nu(E, p) = 0$  whenever this is not the case. We further restrict ourselves to the class of solutions having:

$$\tilde{\psi}_L^{\text{red}}(E, p) = \tilde{\psi}_R^{\text{blue}}(E, p) = 0$$

In the direct space, this just means we focus on wave functions of the form:

$$\psi^\nu(n, k) = \psi_R^{\text{red}}(n, k) |+0\rangle + \psi_L^{\text{blue}}(n, k) |-1\rangle,$$

where  $\psi_R^{\text{red}}(n, k)$  and  $\psi_L^{\text{blue}}(n, k)$  are Fourier conjugates of  $\tilde{\psi}_R^{\text{red}}(E, p)$  and  $\tilde{\psi}_L^{\text{blue}}(E, p)$  respectively. The point is that for  $m = 0$ ,  $\hat{U}_{FQW}^1$  preserves chirality and does not allow  $\psi^\nu(n, k)$ , to be excited to  $\psi_L^{\text{red}}(n, k) |-0\rangle$  or  $\psi_R^{\text{blue}}(n, k) |+1\rangle$ . In other words, the restriction to the sector of right-hand fermions of charge  $0$  and left-hand fermions of charge  $-1$  is stable under the equations of motions. Then we conclude that  $(1+1)$ -D FQW does contain neutrino-like particle solutions.

## 7 Closing remarks

*Technical summary.* In this paper, we analyse and fix Fermion Doubling (FD) for Quantum Cellular Automata (QCA).

The analysis works by writing the equations of motions of the one step evolution of QCA for a single particle in Fourier space and analysing its characteristic polynomial. Due to its cos and sin function, this characteristic polynomial has periodicities, leading to spurious solutions that survive even at arbitrarily small  $\varepsilon$ , and the become ill-defined when  $\varepsilon = 0$ . They are therefore unphysical as they do not belong to the continuum theory, but they will remain their and pollute the numerics even when we increase the precision. We pinpoint the problem at the level of the propagator of the QCA.

The  $(1+1)$  and  $(3+1)$ -QED QCA models of [5, 14] do suffer the FD problem. We show that the number of spurious solutions that are present in the QCA models are half the number of those of the usual lattice fermions Hamiltonian. We show that these doublers appear in a different location of the Brouillon zone (BZ), which explains why they had remained oblivious to prior analysis [5].

We develop a cutting and pasting procedure on the BZ, which we formalize as the application of a covering maps upon the complexification of the BZ. The several sheets of new BZ correspond to flavouring sublattices partitioning direct space. Overall the number of solutions is preserved by this FD fixing procedure, but the previously unphysical solutions have become physical solutions of different flavours. We call this solution *flavouring-without-staggering*. We implement is in full details for the  $(1+1)$  and  $(3+1)$ -QED QCA, resulting in FD-free  $\mathbb{Z}_2$  and  $\mathbb{Z}_2 \times \mathbb{Z}_2 \times \mathbb{Z}_2$  flavoured versions of them. We prove that it still enjoys chiral symmetry.

We discuss misconceptions that surround the the Nielsen-Ninomiya no-go theorem, and why it does not imply that FD solutions break chirality. It does demands that the number of left-handed and right-handed particles per charge and per flavour be the same in a larger Hilbert. Still we show that restricting to a sector of the larger Hilbert space, based on the flavouring structure, leaves room to simulate neutrino-like particles.

*Perspectives.* The Nielsen-Ninomiya no-go theorem is of great importance for our understanding the nature of spacetime—it deserves a modern overhaul. We would also like to better understand the physical interpretation of the flavour symmetries that FD fixing introduces. To some extent they are physical, as they make sure that the discrete model matches the continuum. But could they be recycled encode, or even justify the existence of different particle types, e.g. in order to recover weak interactions?

**Acknowledgments.** This project/publication was made possible through the support of the ID# 62312 grant from the John Templeton Foundation, as part of the ‘[The Quantum Information Structure of Spacetime](#)’ Project (QISS). The opinions expressed in this project/publication are those of the author(s) and do not necessarily reflect the views of the John Templeton Foundation. This work has also been funded by the French National Research Agency (ANR): project TaQC ANR-22-CE47-0012 and within the framework of “Plan France 2030”, under the research projects EPIQ ANR-22-PETQ-0007, OQULUS ANR-23-PETQ-0013, HQI-Acquisition ANR-22-PNCQ-0001 and HQI-R&D ANR-22-PNCQ-0002.

## References

- [1] P. Arrighi, V. Nesme, and M. Forets. The dirac equation as a quantum walk: higher dimensions, observational convergence. *Journal of Physics A: Mathematical and Theoretical*, 47(46):465302, 2014.
- [2] P. Arrighi, V. Nesme, and R. Werner. Unitarity plus causality implies localizability. *J. of Computer and Systems Sciences*, 77:372–378, 2010. Local proceedings of QIP 2010 (long talk).
- [3] P. Arrighi and C. Patricot. A note on the correspondence between qubit quantum operations and special relativity. *Journal of Physics A: Mathematical and General*, 36(20):L287–L296, 2003.
- [4] Pablo Arrighi. An overview of quantum cellular automata. *Natural Computing*, 18:885, 2019. arXiv preprint arXiv:1904.12956.
- [5] Pablo Arrighi, Cédric Bény, and Terry Farrelly. A quantum cellular automaton for one-dimensional qed. *Local proceedings of AQIS 2019. Quantum Information Processing*, 19:88, 2020. arXiv preprint arXiv:1903.07007.
- [6] Pablo Arrighi, Vincent Nesme, and Marcelo Forets. The dirac equation as a quantum walk: higher dimensions, observational convergence. *Journal of Physics A: Mathematical and Theoretical*, 47(46):465302, November 2014.
- [7] T. Banks, S. Raby, L. Susskind, J. Kogut, D. R. T. Jones, P. N. Scharbach, and D. K. Sinclair. Strong-coupling calculations of the hadron spectrum of quantum chromodynamics. *Phys. Rev. D*, 15:1111–1127, Feb 1977.
- [8] Mari Carmen Bañuls, Rainer Blatt, Jacopo Catani, Alessio Celi, Juan Ignacio Cirac, Marcello Dalmonte, Leonardo Fallani, Karl Jansen, Maciej Lewenstein, Simone Montangero, Christine A Muschik, Benni Reznik, Enrique Rico, Luca Tagliacozzo, Karel Van Acoleyen, Frank Verstraete, Uwe-Jens Wiese, Matthew Wingate, Jakub Zakrzewski, and Peter Zoller. Simu-

lating lattice gauge theories within quantum technologies. *The European Physical Journal D*, 74(8):165, August 2020.

- [9] A. Bibeau-Delisle, A. Bisio, G. M. D’Ariano, P. Perinotti, and A. Tosini. Doubly special relativity from quantum cellular automata. *EPL (Europhysics Letters)*, 109(5):50003, 2015.
- [10] Alessandro Bisio, Nicola Mosco, and Paolo Perinotti. Scattering and perturbation theory for discrete-time dynamics. *Physical Review Letters*, 126(25):250503, 2021.
- [11] Fabrice Debbasch. Action principles for quantum automata and lorentz invariance of discrete time quantum walks. *arXiv preprint arXiv:1806.02313*, 2018.
- [12] F. Diamond and J. Shurman. *A First Course in Modular Forms*. Graduate Texts in Mathematics. Springer New York, 2006.
- [13] E.N. Economou. *Green’s Functions in Quantum Physics*. Springer Series in Solid-State Sciences. Springer, 2006.
- [14] Nathanaël Eon, Giuseppe Di Molfetta, Giuseppe Magnifico, and Pablo Arrighi. A relativistic discrete spacetime formulation of  $3+1$  qed. *Quantum*, 7:1179, 2023.
- [15] Terry Farrelly. A review of quantum cellular automaton. *to appear on the arXiv*, 2019.
- [16] R. P. Feynman. Quantum mechanical computers. *Foundations of Physics (Historical Archive)*, 16(6):507–531, 1986.
- [17] D. Friedan. A proof of the Nielsen-Ninomiya theorem. *Commun. Math. Phys.*, 85:481–490, 1982.
- [18] B. Gilligan and O. Forster. *Lectures on Riemann Surfaces*. Graduate Texts in Mathematics. Springer New York, 2012.
- [19] Paul H. Ginsparg and Kenneth G. Wilson. A remnant of chiral symmetry on the lattice. *Phys. Rev. D*, 25:2649–2657, May 1982.
- [20] S. L. Glashow. Partial Symmetries of Weak Interactions. *Nucl. Phys.*, 22:579–588, 1961.
- [21] Brian C. Hall. *Quantum Theory for Mathematicians*. Number 267 in Graduate Texts in Mathematics. Springer New York.
- [22] Nicolas Jolly and Giuseppe Di Molfetta. Twisted quantum walks, generalised dirac equation and fermion doubling. *The European Physical Journal D*, 77(5):80, May 2023.
- [23] Charles Kittel. *Introduction to Solid State Physics*. Wiley, 8 edition, 2004.
- [24] John Kogut and Leonard Susskind. Hamiltonian formulation of wilson’s lattice gauge theories. *Phys. Rev. D*, 11:395–408, Jan 1975.
- [25] Seth Lloyd. Universal quantum simulators. *Science*, 273(5278):1073–1078, 1996.
- [26] M. E. Peskin and D. V. Schroeder. *An Introduction To Quantum Field Theory*. CRC Press, Boca Raton, 1995.
- [27] Esteban A Martinez, Christine A Muschik, Philipp Schindler, Daniel Nigg, Alexander Erhard, Markus Heyl, Philipp Hauke, Marcello Dalmonte, Thomas Monz, Peter Zoller, and Rainer Blatt. Real-time dynamics of lattice gauge theories with a few-qubit quantum computer. *Nature*, 534(7608):516–519, June 2016.
- [28] H. B. Nielsen and M. Ninomiya. A no-go theorem for regularizing chiral fermions. *Phys. Lett. B*, 105(2-3):219–223, 1981.
- [29] H.B. Nielsen and M. Ninomiya. Absence of neutrinos on a lattice: (I). Proof by homotopy theory. *Nuclear Physics B*, 185(1):20–40, 1981.
- [30] H.B. Nielsen and M. Ninomiya. Absence of neutrinos on a lattice: (II). Intuitive topological proof. *Nuclear Physics B*, 193(1):173–194, 1981.
- [31] H. J. Rothe. *Lattice gauge theories: An introduction*. World Scientific, 2005.
- [32] Abdus Salam. Weak and Electromagnetic Interactions. *Conf. Proc. C*, 680519:367–377, 1968.
- [33] Kevissen Sellapillay, Pablo Arrighi, and Giuseppe Di Molfetta. A discrete relativistic spacetime formalism for  $1+1$ -qed with continuum limits. *Scientific Reports*, 12(1):2198, 2022.
- [34] H.S. Sharatchandra, H.J. Thun, and P. Weisz. Susskind fermions on a euclidean lattice. *Nuclear Physics B*, 192(1):205–236, 1981.
- [35] Jan Smit. *Introduction to Quantum Fields on a Lattice*. Cambridge Lecture Notes in Physics. Cambridge University Press, 2023.
- [36] Leonard Susskind. Lattice fermions. *Phys. Rev. D*, 16:3031–3039, Nov 1977.
- [37] Lorenzo Siro Trezzini, Alessandro Bisio, and Paolo Perinotti. Renormalisation of quantum cellular automata, 2024.

- [38] A. Vanrietvelde, O. Mestoudjian, and P. Arrighi. Quantum cellular automata over finite, unbounded configurations. In *Causalworlds 2024, Waterloo*. Local proceedings only, 2024.
- [39] K. G. Wilson. Confinement of quarks. *Phys. Rev. D*, 10:2445–2459, 1974.
- [40] Kenneth G. Wilson. Confinement of quarks. *Phys. Rev. D*, 10:2445–2459, Oct 1974.
- [41] Kenneth G. Wilson. Quarks and Strings on a Lattice. In *13th International School of Subnuclear Physics: New Phenomena in Subnuclear Physics*, 11 1975.

## A Lattice derivatives and hermicity

We are interested in translating hermicity properties from the continuum to the discrete. In this section the stage is  $(1 + 1)$ -dimensional space-time  $\mathcal{M}$ , with boundaries. The continuum, the quantum field we consider is  $\psi : \mathcal{M} \rightarrow \mathbb{C}^2$ , with boundary conditions

$$\psi(t, x) = 0 \text{ at } \partial\mathcal{M}, \quad (\text{A.1})$$

Then the operator  $i\partial_x$  is Hermitian. This statement can be proven by the using the inner product defined for the Dirac fields, which is the integration over the space parameterization of the Lorentz scalar,  $\psi^\dagger \psi$ . Indeed recall that

$$\begin{aligned} & \int dx \psi^\dagger(t, x) (i\partial_x \psi(t, x)) \\ &= \int dx (i\partial_x (\psi^\dagger(t, x) \psi(t, x)) - i\partial_x \psi^\dagger(t, x) \psi(t, x)) \\ &= i(\psi^\dagger(t, x) \psi(t, x))|_{\partial\mathbb{M}} - \int dx (i\partial_x \psi^\dagger(t, x)) \psi(t, x) \\ &= \int dx (i\partial_x \psi(t, x))^\dagger \psi(t, x). \end{aligned} \quad (\text{A.2})$$

Consider discretization of Sec. 2, with boundary conditions

$$\psi(n_i, k) = \psi(n_f, k) = \psi(n, k_i) = \psi(n, k_f) = 0, \quad (\text{A.3})$$

Let us check if forward finite differences keep hermicity.

$$i\partial_x \psi(t, x) \rightarrow \frac{i}{\epsilon} (\psi(n, m + \epsilon) - \psi(n, m)) \quad (\text{A.4})$$

We wish for:

$$\begin{aligned} & \epsilon \sum_{n=n_i, k=k_i}^{n_f, k_f} \psi^\dagger(n, k) \left( \frac{i}{2\epsilon} (\psi(n, k+1) - \psi(n, k)) \right) \\ &= \epsilon \sum_{n=n_i, k=k_i}^{n_f, k_f} \left( \frac{i}{2\epsilon} (\psi(n, k+1) - \psi(n, k)) \right)^\dagger \psi(n, k). \end{aligned} \quad (\text{A.5})$$

We try to manipulate the left hand side of the equation above and use boundary conditions to prove the equality,

$$\begin{aligned}
& \epsilon \sum_{n=n_i, k=k_i}^{n_f, k_f} \psi^\dagger(n, k) \left( \frac{i}{\epsilon} (\psi(n, k+1) - \psi(n, k)) \right) \\
&= i \sum_{n=n_i, k'=k_i+1}^{n_f, k_f+1} \psi^\dagger(n, k'-1) \psi(n, k') - i \sum_{n=n_i, k=k_i}^{n_f, k_f} \psi^\dagger(n, k) \psi(n, k) \\
&= \sum_{n=n_i, k=k_i}^{n_f, k_f} (-i(\psi^\dagger(n, k) - \psi^\dagger(n, k-1))\psi(n, k) \\
&\quad + i\psi^\dagger(n, k_f)\psi(n, k_f+1) - i\psi^\dagger(n, k_i-1)\psi(n, k_i)) \\
&= \epsilon \sum_{n=n_i, k=k_i}^{n_f, k_f} \left( \frac{i}{\epsilon} (\psi(n, k) - \psi(n, k-1))^\dagger \psi(n, k) \right) \\
&\neq \epsilon \sum_{n=n_i, k=k_i}^{n_f, k_f} \left( \frac{i}{\epsilon} (\psi(n, k+1) - \psi(n, k))^\dagger \psi(n, k) \right)
\end{aligned} \tag{A.6}$$

i.e. hermicity is broken. We can replace derivation with symmetric finite differences, and check if it keeps hermicity instead. We want

$$\begin{aligned}
& \epsilon \sum_{n=n_i, k=k_i}^{n_f, k_f} \psi^\dagger(n, k) \left( \frac{i}{2\epsilon} (\psi(n, k+1) - \psi(n, k-1)) \right) \\
&= \epsilon \sum_{n=n_i, k=k_i}^{n_f, k_f} \left( \frac{i}{2\epsilon} (\psi(n, k+1) - \psi(n, k-1)) \right)^\dagger \psi(n, k).
\end{aligned} \tag{A.7}$$

One can rewrite the left hand side of the equation above as,

$$\begin{aligned}
& \frac{i}{2} \sum_{n=n_i, k'=k_i+1}^{n_f, k_f+1} \psi^\dagger(n, k'-1) \psi(n, k') \\
& - \frac{i}{2} \sum_{n=n_i, k''=k_i-1}^{n_f, k_f-1} \psi^\dagger(n, k''+1) \psi(n, k'') \\
&= -\frac{i}{2} \sum_{n=n_i, k=k_i}^{n_f, k_f} (\psi^\dagger(n, k+1) - \psi^\dagger(n, k-1))\psi(n, k) \\
&\quad + \frac{i}{2} \psi^\dagger(n, k_f)\psi(n, k_f+1) - \frac{i}{2} \psi^\dagger(n, k_i)\psi(n, k_i-1) \\
&\quad - \frac{i}{2} \psi^\dagger(n, k_i-1)\psi(n, k_i) + \frac{i}{2} \psi^\dagger(n, k_f+1)\psi(n, k_f) \\
&= \epsilon \sum_{n=n_i, k=k_i}^{n_f, k_f} \left( \frac{i}{2\epsilon} (\psi(n, k+1) - \psi(n, k-1)) \right)^\dagger \psi(n, k),
\end{aligned} \tag{A.8}$$

on the last line of the equation above, we used the boundary conditions that we introduced in Eq. (2.6). We have proved that hermicity of  $i\partial_x$  is preserved by replacing it with symmetric finite differences. The same proof can be done for  $i\partial_t$ .

## B Fourier transformation of the naive discretization scheme

The Dirac vector  $\psi(n, k)$  that we introduced in the section 2, is bounded by the following equation,

$$\epsilon^2 \sum_{n=-\infty}^{\infty} \sum_{k=-\infty}^{\infty} \psi(n, k) \psi^\dagger(n, k) \leq 1. \tag{B.1}$$

Hence we observe that the dimension of  $\psi(n, k)$  is  $\epsilon^{-1}$ . This also can be assured by the definition of  $\tilde{\psi}(E, p)$  because  $\tilde{\psi}(E, p)$  is dimensionless hence the integral form of  $\psi(n, k)$  in the Eq. (2.6) is in the order of  $\epsilon^{-1}$ . This fact can simply proven by the following consistency computations,

$$\begin{aligned}\psi(n, k) &= \epsilon \int_{-\pi/\epsilon}^{\pi/\epsilon} \frac{dE}{2\pi} \int_{-\pi/\epsilon}^{\pi/\epsilon} \frac{dp}{2\pi} \tilde{\psi}(E, p) e^{-ipk\epsilon - iEn\epsilon}, \\ \psi(n, k) &= \epsilon^2 \sum_{n=-\infty}^{\infty} \sum_{k=-\infty}^{\infty} \int_{-\pi/\epsilon}^{\pi/\epsilon} \frac{dE}{2\pi} \int_{-\pi/\epsilon}^{\pi/\epsilon} \frac{dp}{2\pi} \psi(n, k) e^{ip(k-k')\epsilon - iE(n-n')\epsilon} \\ &= \sum_{n=-\infty}^{\infty} \sum_{k=-\infty}^{\infty} \psi(n, k) \delta_{n, n'} \delta_{k, k'} = \psi(n, k). \quad (\text{B.2})\end{aligned}$$

The integral form of  $\psi(n, k)$  is very useful such that we obtained the Eq. (2.6) from that, here is the full calculation,

$$\begin{aligned}& \frac{i\mathbb{I}_2}{2\epsilon} (\psi(n+1, k) - \psi(n-1, k)) + \frac{\sigma_3}{2\epsilon} (\psi(n, k+1) - \psi(n, k-1)) - m\sigma_1 \psi(n, k) \\ &= \epsilon \int_{-\pi/\epsilon}^{\pi/\epsilon} \frac{dE}{2\pi} \int_{-\pi/\epsilon}^{\pi/\epsilon} \frac{dp}{2\pi} \left( \frac{i\mathbb{I}_2}{2\epsilon} (e^{ipk\epsilon - iE(n+1)\epsilon} - e^{ipk\epsilon - iE(n-1)\epsilon}) \tilde{\psi}(E, p) \right. \\ & \quad \left. + \frac{\sigma_3}{2\epsilon} (e^{ip(k+1)\epsilon - iEn\epsilon} - e^{ip(k-1)\epsilon - iEn\epsilon}) \tilde{\psi}(E, p) + -m\sigma_1 e^{ipk\epsilon - iEn\epsilon} \tilde{\psi}(E, p) \right) \\ &= \epsilon \int_{-\pi/\epsilon}^{\pi/\epsilon} \frac{dE}{2\pi} \int_{-\pi/\epsilon}^{\pi/\epsilon} \frac{dp}{2\pi} \left( \frac{i\mathbb{I}_2}{2\epsilon} (e^{-iE(n+1)\epsilon} - e^{-iE(n-1)\epsilon}) \right. \\ & \quad \left. \frac{i\sigma_3}{2\epsilon} (e^{ip(n+1)\epsilon} - e^{ip(n-1)\epsilon}) - m\sigma_1 \right) e^{ipk\epsilon - iEn\epsilon} \tilde{\psi}(E, p) \\ &= \int_{-\pi/\epsilon}^{\pi/\epsilon} \frac{dE}{2\pi} \int_{-\pi/\epsilon}^{\pi/\epsilon} \frac{dp}{2\pi} (\mathbb{I}_2 \sin(E\epsilon) - \sigma_3 \sin(p\epsilon) - m\sigma_1) \tilde{\psi}(E, p) e^{ipk\epsilon - iEn\epsilon} = 0. \quad (\text{B.3})\end{aligned}$$

From the equation above, we conclude that the integrand should be zero, hence we obtain,

$$(\mathbb{I}_2 \sin(E\epsilon) - \sigma_3 \sin(p\epsilon) - m\sigma_1) \tilde{\psi}(E, p) = 0. \quad (\text{B.4})$$

## C From Direct to Fourier lattice vectors

In this paper, we are interested in the BZ of *two-dimensional* and *four-dimensional* direct space lattices, i.e. the integration domains of the Fourier expansion of functions over these lattices. A 2D direct space lattice embeds in a 3D direct space lattice. The 3D lattice is constructed by selecting a discrete, additive subset of  $\mathbb{R}^3$ , such that for any vector in the 3D lattice  $\Lambda^3 \subset \mathbb{R}^3$  is

$$n_1 \vec{a}_1 + n_2 \vec{a}_2 + n_3 \vec{a}_3, \quad (\text{C.1})$$

where  $n_1, n_2, n_3 \in \mathbb{Z}$  and  $\vec{a}_1, \vec{a}_2, \vec{a}_3$  are vectors in  $\mathbb{R}^3$ , they are called lattice vectors. We do have translational symmetry, such that moving integer times of  $\vec{a}_1, \vec{a}_2, \vec{a}_3$  is equal to not moving. This translation invariance definitely puts a bound on the Fourier space since momentum defined to be the generator of translation symmetry. We define reciprocal lattice vectors, that can be seen as lattice vectors on Fourier space, as follows.

$$\begin{aligned}\vec{k}_1 &= 2\pi \frac{a_2 \wedge a_3}{a_1 \cdot (a_2 \wedge a_3)} \\ \vec{k}_2 &= 2\pi \frac{a_3 \wedge a_1}{a_1 \cdot (a_2 \wedge a_3)} \\ \vec{k}_3 &= 2\pi \frac{a_1 \wedge a_2}{a_1 \cdot (a_2 \wedge a_3)},\end{aligned} \quad (\text{C.2})$$

where  $\wedge$  is the usual exterior product on  $\mathbb{R}^3$ . From the definitions above, we should also have  $\vec{a}_i \cdot \vec{k}_j = 2\pi\delta_{ij}$ . Note that  $-\vec{k}_1, \vec{k}_2, \vec{k}_3$  are as well reciprocal lattice vectors. Then the BZ is defined by the Bragg equation [23] which actually can be written as

$$2\vec{p} \cdot \vec{k} = k \cdot \vec{k} \quad (\text{C.3})$$

where  $\vec{k} = n_1\vec{k}_1 + n_2\vec{k}_2 + n_3\vec{k}_3$ ,  $n_1, n_2, n_3 \in \mathbb{Z}$ ,  $|n_1 + n_2 + n_3| \leq 1$  and  $\vec{p}$  is the vector in Fourier space that characterises the BZ which has been bounded by the equation above. Namely, the boundary of the BZ is the minimal compact subset of the set that contains all the possible  $\vec{p}$  that solves Eq. (C.3). Note that conventionally a BZ is constructed by the intersection of planes that cut orthogonally each of the reciprocal lattice vectors and its additive inverses into two equal pieces.

### C.1 A 2-Dimensional Oblique Lattice

In the paper we used  $\{\vec{x}, \vec{y}, \vec{z}\}$  as the orthonormal base for  $\mathbb{R}^3$ . By setting the lattice spacing to  $\epsilon$ , we define the oblique lattice vectors

$$\begin{aligned} \vec{a}_1 &= \epsilon(\vec{y} - \vec{x}) \\ \vec{a}_2 &= \epsilon(\vec{x} + \vec{y}) \\ \vec{a}_3 &= \epsilon\vec{z}, \end{aligned} \quad (\text{C.4})$$

and the reciprocal lattice vectors are

$$\begin{aligned} \vec{k}_1 &= \frac{\pi}{\epsilon}(\vec{x} - \vec{y}) \\ \vec{k}_2 &= -\frac{\pi}{\epsilon}(\vec{y} + \vec{x}) \\ \vec{k}_3 &= \frac{2\pi}{\epsilon}\vec{z}. \end{aligned} \quad (\text{C.5})$$

Since the  $z$ th component of the three dimensional lattice is independent, we disregard it, and we reduce the dimension of the lattice to two with lattice vectors  $\vec{a}_1, \vec{a}_2$  and reciprocal lattice vectors  $\vec{k}_1, \vec{k}_2$ . Hence Eq. (C.3) for  $\vec{p} = p_x\vec{x} + p_y\vec{y}$  becomes

$$(n_1 - n_2)p_x - (n_2 + n_1)p_y = \frac{\pi}{\epsilon}(n_1^2 + n_2^2). \quad (\text{C.6})$$

We obtain 4 possible solutions, yielding the minimal region,

$$p_x - p_y = \frac{\pi}{\epsilon} \quad (\text{C.7a})$$

$$-p_x + p_y = \frac{\pi}{\epsilon} \quad (\text{C.7b})$$

$$-p_x - p_y = \frac{\pi}{\epsilon} \quad (\text{C.7c})$$

$$p_x + p_y = \frac{\pi}{\epsilon} \quad (\text{C.7d})$$

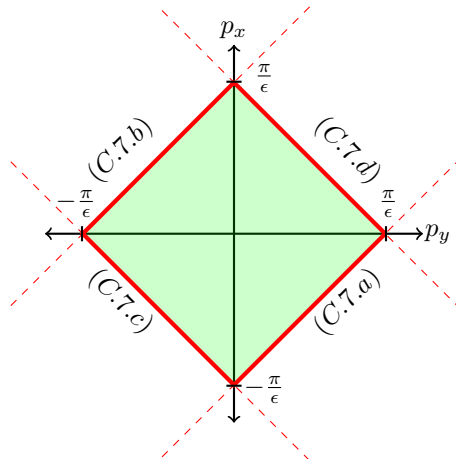


Figure 7: The BZ of the Oblique Lattice

The red lines in the figure 7 1 are unions of the points that solve Eq. eq. (C.7). Hence the set of all possible solutions of Eq. eq. (C.3) forms the boundaries of the BZ. Thus, the BZ of the oblique lattice, that has been defined by Eq. eq. (C.1), is the shaded area in the figure 7. Another way of constructing the BZ of the oblique lattice would be to take the intersection of the four planes that cut the vectors  $\pm\vec{k}_1, \pm\vec{k}_2$ , orthogonally into two pieces. Observe that the line that was described by Eq. eq. (C.7a) cuts orthogonally  $\vec{k}_1$  into two pieces, and Eq. eq. (C.7b) cuts orthogonally  $-\vec{k}_1$  into two pieces. Eq. eq. (C.7d) and Eq. eq. (C.7c) cuts cuts orthogonally  $\vec{k}_2, -\vec{k}_2$  into two pieces respectively. If construction of a BZ is just the intersection of the normal planes of the corresponding reciprocal lattice vectors, why bother with the Bragg equation? The answer is that finding such an intersection is rather difficult in higher dimensional situations.

## C.2 A four dimensional oblique lattice

We are interested in simulations of  $(3+1)$ D space-time in discrete settings which can be realised as 4 dimensional lattices. Let us provide useful facts about lattices in 4 dimensions. In the paper, we use this four-dimensional oblique lattice:

$$\begin{aligned} a_0 &= \epsilon(1, 1, 1, 1), & a_1 &= \epsilon(1, -1, 1, 1) \\ a_2 &= \epsilon(1, 1, -1, 1), & a_3 &= \epsilon(1, 1, 1, -1) \end{aligned} \quad (\text{C.8})$$

We would like to find the reciprocal space of the lattice above. It is constructed by means the vectors below

$$\vec{b}_0 = 2\pi \frac{a_1 \wedge a_2 \wedge a_3}{a_0 \cdot (a_1 \wedge a_2 \wedge a_3)} \quad (\text{C.9a})$$

$$\vec{b}_1 = -2\pi \frac{a_0 \wedge a_2 \wedge a_3}{a_0 \cdot (a_1 \wedge a_2 \wedge a_3)} \quad (\text{C.9b})$$

$$\vec{b}_2 = 2\pi \frac{a_0 \wedge a_1 \wedge a_3}{a_0 \cdot (a_1 \wedge a_2 \wedge a_3)} \quad (\text{C.9c})$$

$$\vec{b}_3 = -2\pi \frac{a_0 \wedge a_1 \wedge a_2}{a_0 \cdot (a_1 \wedge a_2 \wedge a_3)}, \quad (\text{C.9d})$$

$$\begin{aligned} \vec{b}_0 &= \frac{\pi}{\epsilon}(-1, 1, 1, 1), & \vec{b}_1 &= \frac{\pi}{\epsilon}(1, -1, 0, 0) \\ \vec{b}_2 &= \frac{\pi}{\epsilon}(1, 0, -1, 0), & \vec{b}_3 &= \frac{\pi}{\epsilon}(1, 0, 0, -1). \end{aligned} \quad (\text{C.10})$$

Note that for each reciprocal vector above, and its additive inverse, there exists a three-dimensional plane that cuts it orthogonally into two pieces. Intersection of these planes gives the BZ of the four-dimensional oblique lattice. However, it is not straight-forward to study such an intersection. Instead, let use the Bragg equation. We let  $b = l_0\vec{b}_0 + l_1\vec{b}_1 + l_2\vec{b}_2 + l_3\vec{b}_3$  and  $p = (p_0, p_1, p_2, p_3)$ . The BZ of the four dimensional oblique lattice is given by:

$$\begin{aligned} 2p \cdot b - b \cdot b &= -\frac{2\pi}{\epsilon}(p_0(l_1 + l_2 + l_3 - l_0) + p_1(l_0 - l_1) + p_2(l_0 - l_2) + p_3(l_0 - l_3) \\ &\quad + \frac{\pi^2}{\epsilon^2}(2l_0^2 + l_1^2 + l_2^2 + l_2l_3 + l_3^2 + l_1(l_2 + l_3) - 2l_0(l_1 + l_2 + l_3))) = 0. \end{aligned} \quad (\text{C.11})$$

Let us find the constraints on two-dimensional hyper-surfaces of the BZ. There exists 6 distinct two-dimensional hyper-surfaces of the BZ. To describe the BZ projected on a chosen two dimensional hyper-surface, one has to obtain 4 equations as we had in Eq. (C.7). When  $l_0 = l_1 = l_2 = 0$  and  $l_3 = \pm 1$ , Eq. (C.11) becomes

$$p_0 - p_3 = \pm \frac{\pi}{\epsilon}, \quad (\text{C.12})$$

Let us take  $l_0 = l_1 = l_2 = \pm 1$  and  $l_3 = 0$ , we obtain

$$p_0 + p_3 = \pm \frac{\pi}{\epsilon}. \quad (\text{C.13})$$

We continue with the case when  $l_0 = l_1 = l_3 = 0$ ,  $l_2 = \pm 1$ , and the case when  $l_0 = l_1 = l_3 = \pm 1$ ,  $l_2 = 0$ , for two of the cases we obtain the following equations respectively

$$p_0 - p_2 = \pm \frac{\pi}{\epsilon}, \quad (\text{C.14})$$

$$p_0 + p_2 = \pm \frac{\pi}{\epsilon}. \quad (\text{C.15})$$

Similarly, for  $l_0 = l_2 = l_3 = 0$ ,  $l_1 = \pm 1$ , and  $l_0 = l_2 = l_3 = \pm 1$ ,  $l_1 = 0$  we obtain the following equations respectively,

$$p_0 - p_1 = \pm \frac{\pi}{\epsilon}, \quad (\text{C.16})$$

$$p_0 + p_1 = \pm \frac{\pi}{\epsilon}. \quad (\text{C.17})$$

We continue with  $l_0 = \pm 1$ ,  $l_1 = \mp 1$ ,  $l_2 = 0$ ,  $l_3 = \pm 1$ , and  $l_0 = 0$ ,  $l_1 = \mp 1$ ,  $l_2 = \pm 1$ ,  $l_3 = 0$  we obtain the following equations respectively,

$$p_1 + p_2 = \pm \frac{\pi}{\epsilon}, \quad (\text{C.18})$$

$$p_1 - p_2 = \pm \frac{\pi}{\epsilon}. \quad (\text{C.19})$$

For  $l_0 = \pm 1$ ,  $l_1 = \mp 1$ ,  $l_2 = \pm 1$ ,  $l_3 = 0$ , and  $l_0 = 0$ ,  $l_1 = \mp 1$ ,  $l_2 = 0$ ,  $l_3 = \pm 1$  we obtain the following equations respectively,

$$p_1 + p_3 = \pm \frac{\pi}{\epsilon}, \quad (\text{C.20})$$

$$p_1 - p_3 = \pm \frac{\pi}{\epsilon}. \quad (\text{C.21})$$

Finally, when  $l_0 = \pm 1$ ,  $l_2 = l_3 = l_1 = 0$ , and  $l_0 = 0$ ,  $l_1 = 0$ ,  $l_2 = \mp 1$ ,  $l_3 = \pm 1$  we obtain the following equations respectively,

$$p_2 + p_3 = \pm \frac{\pi}{\epsilon}, \quad (\text{C.22})$$

$$p_2 - p_3 = \pm \frac{\pi}{\epsilon}. \quad (\text{C.23})$$

Through the equations above, we observe that projections of the BZ of four dimensional oblique lattice to each hyperplanes,  $p_0 - p_1$ ,  $p_0 - p_2$ ,  $p_0 - p_3$  and  $p_1 - p_2$ ,  $p_1 - p_3$ ,  $p_2 - p_3$  admit a rhombus.

## D A way of representing higher dimensional BZs with two-dimensional BZs

We would like to convey a way of representing the higher dimensional BZs that we are interested in, with the use of two-dimensional BZs that are easy to work with. Our approach will be based on embedding the higher dimensional BZ into a space that is constructed by the Cartesian product of two-dimensional BZs. Let us start with a simple example of three-dimensional BZ. We first describe a three-dimensional BZ in the following Subsec. D.1. After this section, we continue with the four-dimensional oblique lattice in SubSec. D.1.2.

### D.1 Body Centred Cubic Lattice

We give a study of the construction of the BZ of body centered cubic lattice which has the following lattice vectors,

$$\begin{aligned} \vec{a}_1 &= \epsilon(\hat{y} - \hat{x} + \hat{z}) \\ \vec{a}_2 &= \epsilon(-\hat{y} + \hat{x} + \hat{z}) \\ \vec{a}_3 &= \epsilon(\hat{y} + \hat{x} - \hat{z}), \end{aligned} \quad (\text{D.1})$$

and whose reciprocal lattice vectors are

$$\begin{aligned}\vec{k}_1 &= \frac{\pi}{\epsilon}(\hat{z} + \hat{y}) \\ \vec{k}_2 &= \frac{\pi}{\epsilon}(\hat{z} + \hat{x}) \\ \vec{k}_3 &= \frac{\pi}{\epsilon}(\hat{x} + \hat{y}).\end{aligned}\tag{D.2}$$

We observe that, the body centred cubic lattice cannot be reduced to two dimensions as we did for the BZ of the two-dimensional oblique lattice, where  $\vec{k}_3 = \hat{z}$ . However, for this case, the first Brillouin zone is a volume whose boundary has been constructed by the possible  $\vec{p} = p_x\hat{x} + p_y\hat{y} + p_z\hat{z}$  which should obey to Eq. (C.3), hence we obtain

$$p_z(n_1 + n_2) + p_y(n_1 + n_3) + p_x(n_2 + n_3) = \frac{\pi}{2\epsilon}((n_1 + n_2)^2 + (n_1 + n_3)^2 + (n_2 + n_3)^2).\tag{D.3}$$

This gives 12 possible equations for two dimensional surfaces:

$$p_x - p_y = \pm \frac{\pi}{\epsilon}, \quad p_x + p_y = \pm \frac{\pi}{\epsilon}\tag{D.4a}$$

$$p_x - p_z = \pm \frac{\pi}{\epsilon}, \quad p_x + p_z = \pm \frac{\pi}{\epsilon}\tag{D.4b}$$

$$p_y - p_z = \pm \frac{\pi}{\epsilon}, \quad p_y + p_z = \pm \frac{\pi}{\epsilon}\tag{D.4c}$$

Each subequations corresponds a surface in three dimensional Fourier space, by the intersections of them, they bound a region which happens to be regular rhombic dodecahedron. It has 12 faces that corresponds to the solutions of Eq. (D.4) and delete their non-compact parts. We obtain the following figure in three dimensional Fourier space.

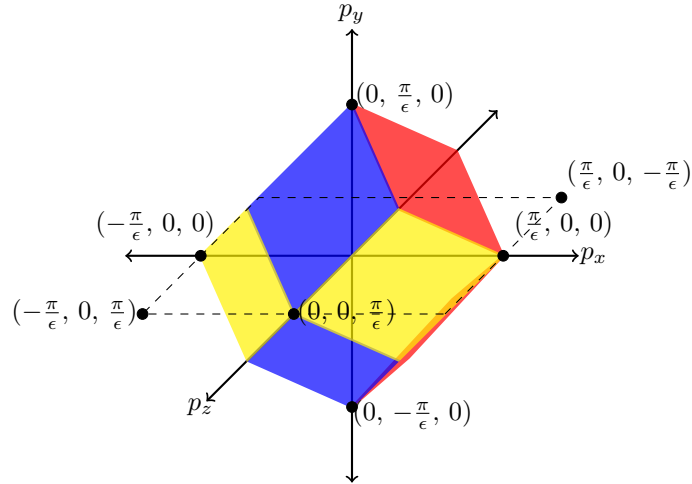


Figure 8: The First Brillouin Zone of the Body centered Cubic Lattice

Red, yellow and blue indicate the solutions of (D.4.a), (D.4.b) and (D.4.c) respectively.

#### D.1.1 Adding a degeneracy

Let us now focus on the  $p_x - p_y$  and  $p_x - p_z$  cross-sections in Fig. 8, and consider them as individual BZs. From Eq. D.4, we know that they are rhombus shaped. Then with using Eq. C.5, we can define the reciprocal vectors for  $p_x - p_y$  and  $p_x - p_z$ , in three dimensions with the unit vectors  $\{\hat{x}, \hat{y}, \hat{z}\}$ . We then let,

$$\begin{aligned}\tilde{b}_1(\hat{x} + \hat{y})\frac{\pi}{\epsilon}, \quad \tilde{b}_2 = (\hat{x} - \hat{y})\frac{\pi}{\epsilon}, \\ \tilde{\tilde{b}}_1 = (\hat{x} + \hat{z})\frac{\pi}{\epsilon}, \quad \tilde{\tilde{b}}_2 = (\hat{x} - \hat{z})\frac{\pi}{\epsilon},\end{aligned}\tag{D.5}$$

where  $\{\tilde{b}_1, \tilde{b}_2\}$  are the reciprocal vectors for  $px - py$ , and  $\{\tilde{\tilde{b}}_1, \tilde{\tilde{b}}_2\}$  are the reciprocal vectors for  $px - pz$ . For the body centred cubic lattice, we had three reciprocal vectors, but right now we have four, did we made mistake? Do these four reciprocal give the same BZ as the body centred cubic lattice? There is only one way of understanding whether the structure that we propose yields the same BZ, as in 8, namely by imposing Eq. C.3. We define  $\tilde{b} = n\tilde{b}_1 + m\tilde{\tilde{b}}_1 + x\tilde{\tilde{b}}_1 + \tilde{\tilde{b}}_2$ , where  $n, m, x, l \in \mathbb{Z}$ . Next we find the minimal region that is determined by  $-2\vec{p} \cdot \tilde{b} + \tilde{b} \cdot \tilde{b}$ . This is

$$(m-n)^2 + (l-x)^2 + (l+m+n+x)^2 - 2((m-n)py + pz(-l+x) + px(l+m+n+x)) = 0 \quad (\text{D.6})$$

For  $m = \pm 1, n = x = l = 0$ ,  $n = \pm 1, m = x = l = 0$ ,  $x = \pm 1, m = n = l = 0$ ,  $l = \pm 1, m = n = x = 0$  we obtain respectively

$$p_x + p_y = \pm \frac{\pi}{\epsilon} \quad (\text{D.7a})$$

$$p_x - p_y = \pm \frac{\pi}{\epsilon} \quad (\text{D.7b})$$

$$p_x + p_z = \pm \frac{\pi}{\epsilon} \quad (\text{D.7c})$$

$$p_x - p_z = \pm \frac{\pi}{\epsilon}. \quad (\text{D.7d})$$

The equations above lead to rhombuses in  $px - py$ ,  $px - pz$ . But we have not yet obtained the relations between  $py - pz$  that were displayed in Eq. (D.4). Let us go further and try the cases  $m = \pm 1, x = \mp 1, n = l = 0$ ,  $n = \mp 1, x = \pm 1, m = l = 0$ , we obtain respectively

$$p_z - p_y = \pm \frac{\pi}{\epsilon} \quad (\text{D.8a})$$

$$p_z + p_y = \pm \frac{\pi}{\epsilon}. \quad (\text{D.8b})$$

The condition that is given in Eq. (C.3) does not see the difference between the reciprocal lattice vectors  $\{\tilde{b}_1, \tilde{b}_1, \tilde{\tilde{b}}_1, \tilde{\tilde{b}}_2\}$  and the reciprocal lattice vectors of body centred cubic lattice. Hence the structure that is constructed by two individual BZs in  $px - py$ ,  $px - pz$  planes is a degenerate solution for the reciprocal lattice vectors of body centred cubic lattice. This degenerative representation is very useful, because now we do not need to study the reciprocal lattice vectors as it is, rather we will focus on a finite number of two-dimensional BZs.

#### D.1.2 Embedding the BZ of body centred cubic lattice into the product of two BZs of oblique lattice.

The BZ of the oblique lattice can be constructed by a quotient topology,  $\mathbb{C}/\Gamma^2$ , where  $p_0 + ip_1 \in \mathbb{C}$ ,  $\Gamma^2$  is spanned by  $(m_0 + n_0)/2 + i(m_0 - n_0)/2$  with  $n_i, m_i \in \mathbb{Z}$ , for every  $i \in \mathbb{Z}$ . Let us consider  $\mathbb{C}/\Gamma^2 \times \mathbb{C}/\Gamma^2$ , which has coordinates  $(p_0 + ip_1, p_2 + ip_3)$ . Note that  $(p_0 + ip_1)$  has translational symmetry with respect to the lattice  $(m_0 + n_0)/2 + i(m_0 - n_0)/2$ , and  $(p_2 + ip_3)$  has translational symmetry with respect to the lattice  $(m_1 + n_1)/2 + i(m_1 - n_1)/2$ .

To obtain the BZ of body centred cubic lattice, from  $\mathbb{C}/\Gamma^2 \times \mathbb{C}/\Gamma^2$ , we define a projection map,  $\rho : \mathbb{C}^2 \rightarrow R^3$ , by the identification,  $p_0 = p_2$ , which constraints on the level of the lattices, hence this identification makes  $m_1 = m_0 + n_0 - n_1$ . Then the projection map induces a map  $\Phi^*$  on  $\Gamma^2 \times \Gamma^2$ , such that,

$$\begin{aligned} \Phi^*((m_0 + n_0)/2 + i(m_0 - n_0)/2, (m_1 + n_1)/2 + i(m_1 - n_1)/2) \\ = ((m_0 + n_0)/2, (m_0 - n_0)/2, (m_0 + n_0)/2 - n_1). \end{aligned} \quad (\text{D.9})$$

The projection map is defined to be

$$\pi : \mathbb{C}/\Gamma^2 \times \mathbb{C}/\Gamma^2 \rightarrow R^3/\Phi^*(\Gamma^2 \times \Gamma^2). \quad (\text{D.10})$$

## D.2 Four-dimensional oblique lattice

### D.2.1 Adding a degeneracy

Instead of the reciprocal lattice vectors in Eq. (C.9), we will use the following reciprocal lattice vectors for the four-dimensional oblique lattice,

$$\begin{aligned}\tilde{b}_0^x &= (\hat{E} + \hat{p}_x) \frac{\pi}{\epsilon}, & \tilde{b}_1^x &= (\hat{E} - \hat{p}_x) \frac{\pi}{\epsilon} \\ \tilde{b}_0^y &= (\hat{E} + \hat{p}_y) \frac{\pi}{\epsilon}, & \tilde{b}_1^y &= (\hat{E} - \hat{p}_y) \frac{\pi}{\epsilon} \\ \tilde{b}_0^z &= (\hat{E} + \hat{p}_z) \frac{\pi}{\epsilon}, & \tilde{b}_1^z &= (\hat{E} - \hat{p}_z) \frac{\pi}{\epsilon},\end{aligned}\tag{D.11}$$

where  $\{\hat{E}, \hat{p}_x, \hat{p}_y, \hat{p}_z\}$  is a choice of orthogonal coordinate system in  $\mathbb{R}^4$ . We define  $\tilde{\tilde{b}} = n_0^x \tilde{b}_0^x + n_1^x \tilde{b}_1^x + n_0^y \tilde{b}_0^y + n_1^y \tilde{b}_1^y + n_0^z \tilde{b}_0^z + n_1^z \tilde{b}_1^z$ , where  $n_j^i \in \mathbb{Z}$  for every  $i \in \{x, y, z\}$ ,  $j \in \{0, 1\}$  and  $\mathbf{p} = (E, p_x, p_y, p_z)$ . Then the solution  $2\mathbf{p} \cdot \tilde{\tilde{b}} - \tilde{\tilde{b}} \cdot \tilde{\tilde{b}} = 0$  for arbitrary  $\mathbf{p}$  leads to a minimal volume which is  $\mathcal{B}^{2'}$ . Let us prove that this statement is correct.

$$\begin{aligned}2\mathbf{p} \cdot \tilde{\tilde{b}} - \tilde{\tilde{b}} \cdot \tilde{\tilde{b}} &= \\ &= -\frac{\pi^2}{\epsilon^2} ((n_0^x - n_1^x)^2 - (n_0^y - n_1^y)^2 - (n_0^z - n_1^z)^2 - (n_0^x + n_0^y + n_0^z + n_1^x + n_1^y + n_1^z)^2) \\ &+ \frac{2\pi}{\epsilon} (E(n_0^x + n_0^y + n_0^z + n_1^x + n_1^y + n_1^z) + (n_0^x - n_1^x)p_x + (n_0^y - n_1^y)p_y + (n_0^z - n_1^z)p_z).\end{aligned}\tag{D.12}$$

We compare Eq. (C.11) with Eq. (D.12), we observe that if the following conditions are true,

$$\begin{aligned}n_0^z &= l_0 - n_0^y - n_0^x, & n_1^x &= l_1 + n_0^x \\ n_1^y &= -l_0 + l_2 + n_0^y, & n_1^z &= l_3 - n_0^x - n_0^y,\end{aligned}\tag{D.13}$$

then we find that Eq. (D.12) is the same as Eq. (C.11). Since the  $n_j^i$  are arbitrary integer, the conditions above can be easily realised as they do not violate integer nature of  $n_j^i$ . Eq. (D.12) describes the BZ of 4-dimensional oblique lattice: we can deduce this fact by producing the constraints in Eqs. (C.12)- (C.22) by the use of Eq. (D.13). The table below shows that Eq. (D.12) produces same the constraints as Eq. (C.11), for a chosen set of  $(n_0^x, n_1^x, n_0^y, n_1^y, n_0^z, n_1^z)$ .

$(n_0^x, n_1^x, n_0^y, n_1^y, n_0^z, n_1^z)$	The constraint
$(\pm 1, 0, 0, 0, 0, 0)$	$E + p_x = \pm 1$
$(0, \pm 1, 0, 0, 0, 0)$	$E - p_x = \pm 1$
$(0, 0, \pm 1, 0, 0, 0)$	$E + p_y = \pm 1$
$(0, 0, 0, \pm 1, 0, 0)$	$E - p_y = \pm 1$
$(0, 0, 0, 0, \pm 1, 0)$	$E + p_z = \pm 1$
$(0, 0, 0, 0, 0, \pm 1)$	$E - p_z = \pm 1$
$(\pm 1, 0, 0, \mp 1, 0, 0)$	$p_x + p_y = \pm 1$
$(\pm 1, 0, \mp 1, 0, 0, 0)$	$p_x - p_y = \pm 1$
$(\pm 1, 0, 0, 0, 0, \mp 1)$	$p_x + p_z = \pm 1$
$(\pm 1, 0, 0, 0, \mp 1, 0)$	$p_x - p_z = \pm 1$
$(0, 0, \pm 1, 0, 0, \mp 1)$	$p_y + p_z = \pm 1$
$(0, 0, \pm 1, 0, \mp 1, 0)$	$p_y - p_z = \pm 1$

Hence the reciprocal vectors in Eq. D.11 produce  $\mathcal{B}^{2'}$ .

### D.2.2 Embedding the BZ of the four-dimensional oblique lattice into the product of three BZs of oblique lattice.

Let us embed the reciprocal lattice in Eq. D.11 into  $\mathbb{R}^6$  which has orthogonal unit vectors,  $\{\hat{E}_1, \hat{p}_x, \hat{E}_2, \hat{p}_y, \hat{E}_3, \hat{p}_z\}$ . Eq. D.11 becomes

$$\begin{aligned}
\tilde{b}_0^x &= (\hat{E}_1 + \hat{p}_x) \frac{\pi}{\epsilon}, & \tilde{b}_1^x &= (\hat{E}_1 - \hat{p}_x) \frac{\pi}{\epsilon} \\
\tilde{b}_0^y &= (\hat{E}_2 + \hat{p}_y) \frac{\pi}{\epsilon}, & \tilde{b}_1^y &= (\hat{E}_2 - \hat{p}_y) \frac{\pi}{\epsilon} \\
\tilde{b}_0^z &= (\hat{E}_3 + \hat{p}_z) \frac{\pi}{\epsilon}, & \tilde{b}_1^z &= (\hat{E}_3 - \hat{p}_z) \frac{\pi}{\epsilon}.
\end{aligned} \tag{D.15}$$

If we want to get back to the vectors in Eq. D.11, we only need to apply a simple projection map  $\Pi$  that makes  $E_1 = E_2 = E_3$ . Now we see that we only have two dimensional reciprocal lattice vectors that are independent from each other. Because of this, we get three independent BZs on the planes  $E_1 - p_x$ ,  $E_2 - p_y$ ,  $E_3 - p_z$ . Meaning that the reciprocal lattice vectors in Eq. D.15 generates a product of three rhombus shaped BZs. Hence this BZ can be written as  $\mathcal{B}^3 = \mathbb{C}/\Gamma^2 \times \mathbb{C}/\Gamma^2 \times \mathbb{C}/\Gamma^2$ . When the projection map  $\Pi$  is applied on  $\mathcal{B}^3$ , we get

$$\Pi : \mathbb{C}/\Gamma^2 \times \mathbb{C}/\Gamma^2 \times \mathbb{C}/\Gamma^2 \rightarrow \mathbb{C}^2/\Phi^*(\Gamma^2 \times \Gamma^2 \times \Gamma^2), \tag{D.16}$$

where  $\Phi^* : \Gamma^2 \times \Gamma^2 \times \Gamma^2 \rightarrow \Theta^2$  is the induces map, which outputs a complex lattice  $\Theta^2$ , that is

$$\begin{aligned}
\Phi^*((n_0^x + n_1^x)/2 + i(n_0^x - n_1^x)/2, (n_0^y + n_1^y)/2 + i(n_0^y - n_1^y)/2, (n_0^z + n_1^z)/2 + i(n_0^z - n_1^z)/2) \\
= ((n_0^x + n_1^x)/2 + i(n_0^x - n_1^x)/2, (n_0^x + n_1^x)/2, (1 + i) - (n_1^y + in_1^z)).
\end{aligned} \tag{D.17}$$

From there we deduce that  $\Theta^2 = \Gamma^4$ , hence we prove that  $\Pi(\mathcal{B}^3) = \mathcal{B}^{2'}$ .